

Figure 1.

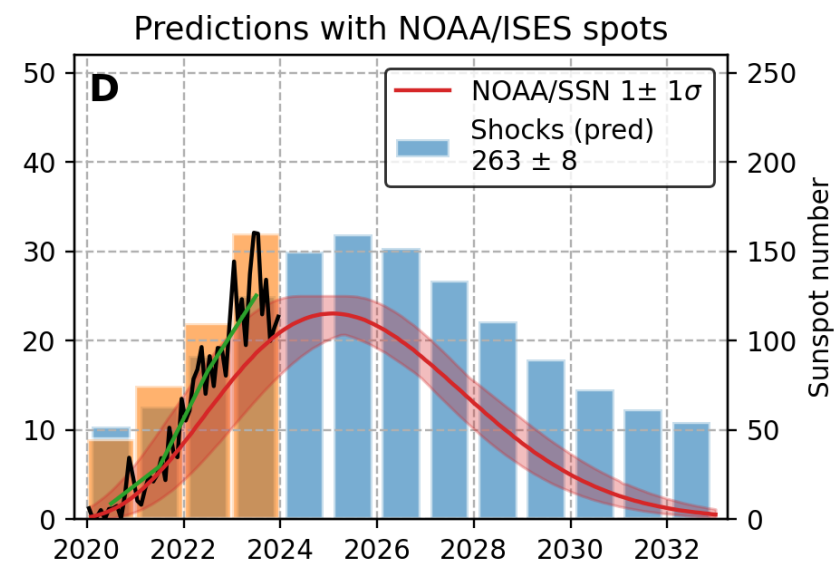
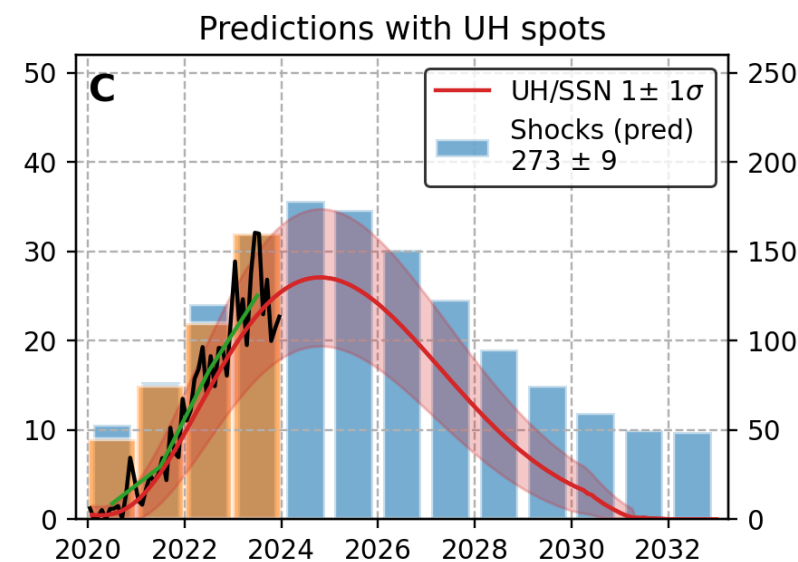
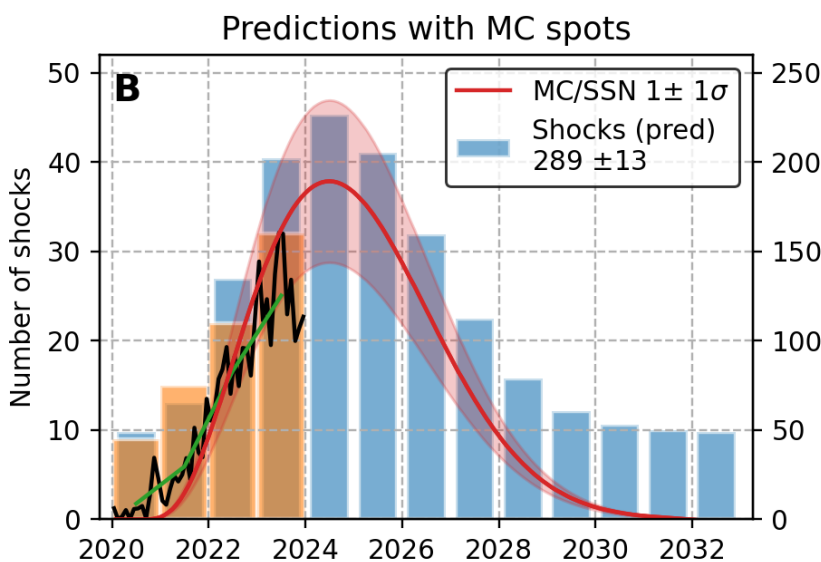
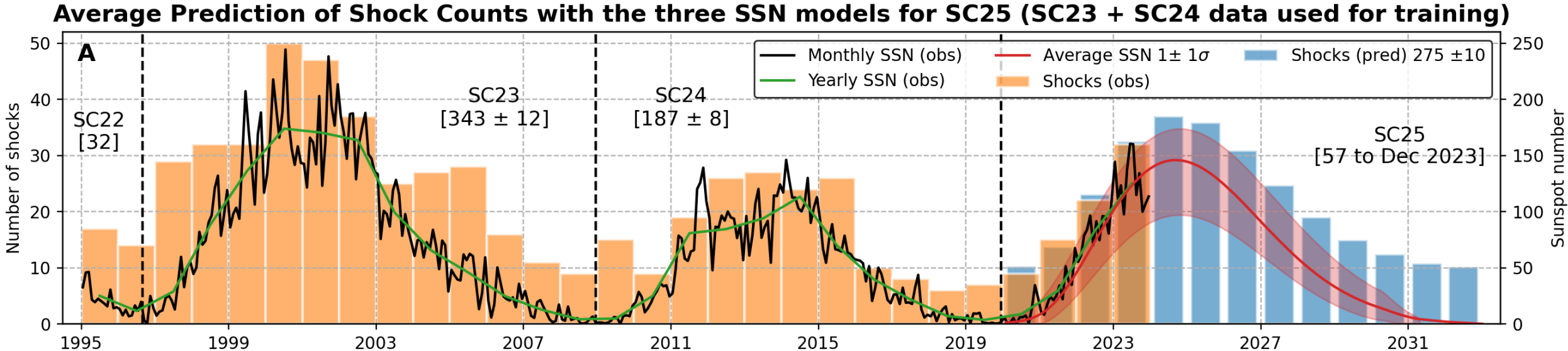
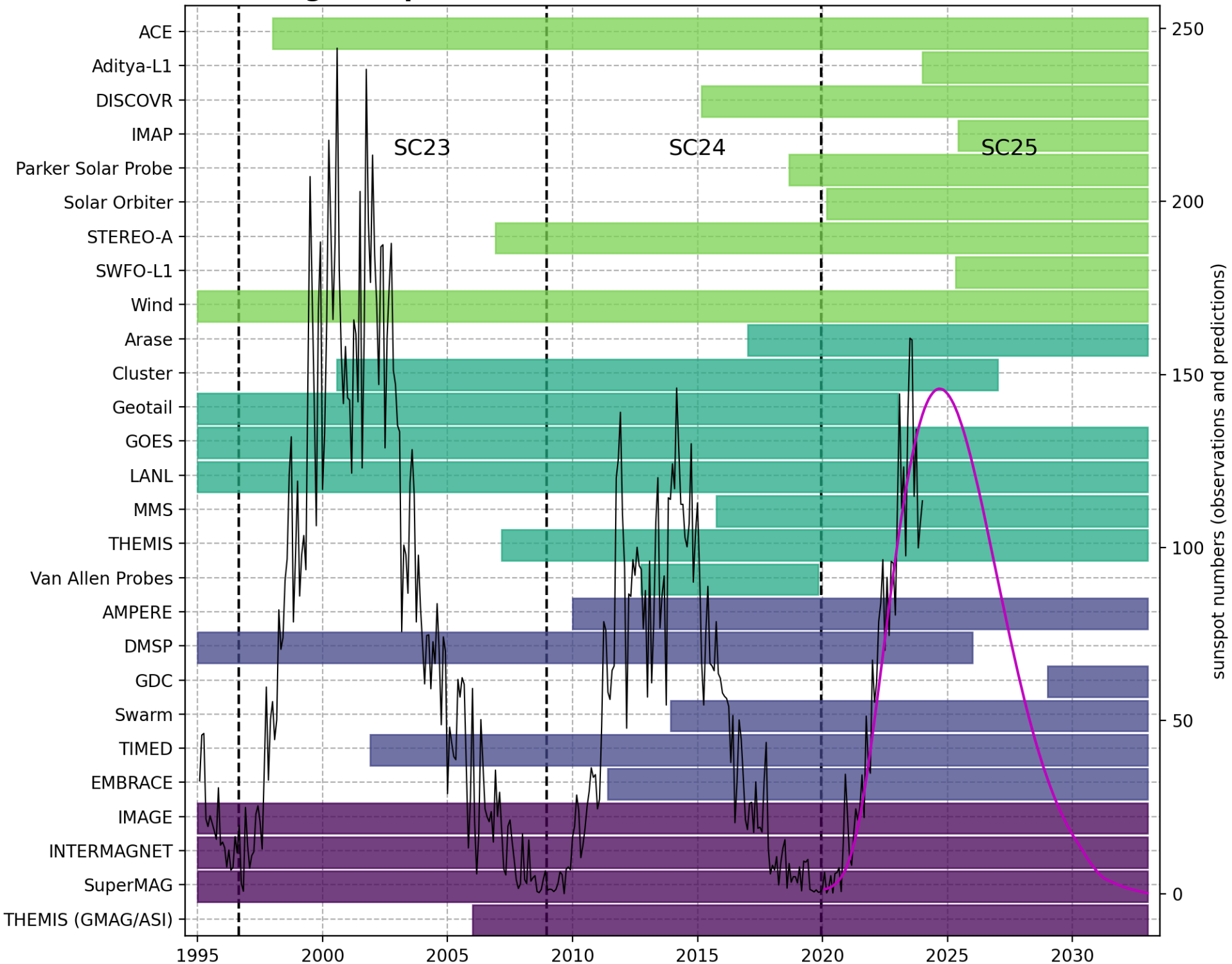


Figure 2.

Ground-, LEO-, magnetosphere-, and solar wind-based data for shock studies



— SSN (obs) — SSN (avg pred) Ground LEO Magnetosphere Solar wind

1
2 **Predicting Interplanetary Shock Occurrence for Solar Cycle 25:**
3 **Opportunities and Challenges in Space Weather Research**
4
5

6 Denny M. Oliveira^{1,2,*}, Robert C. Allen³, Livia R. Alves⁴, Séan P. Blake^{5,6}, Brett A. Carter⁷,
7 Dibyendu Chakrabarty⁸, Giulia D'Angelo^{9,10}, Kevin Delano^{1,2}, Ezequiel Echer⁴, Cristian P.
8 Ferradas^{11,2}, Matt G. Finley^{12,13,2}, Bea Gallardo-Lacourt^{11,2}, Dan Gershman², Jesper W.
9 Gjerloev¹⁴, John Bosco Habarulema¹⁵, Michael D. Hartinger¹⁶, Rajkumar Hajra¹⁷, Hisashi
10 Hayakawa¹⁸, Liisa Juusola¹⁹, Karl M. Laundal²⁰, Robert J. Leamon^{1,2}, Michael Madelaire²⁰,
11 Miguel Martínez-Ledesma^{11,2}, Scott M. McIntosh²¹, Yoshizumi Miyoshi¹⁸, Mark B. Moldwin²²,
12 Emmanuel Nahayo¹⁵, Dibyendu Nandy^{23,24}, Bhosale Nilam²⁵, Katariina Nykyri², William R.
13 Paterson², Mirko Piersanti^{9,10}, Ermanno Pietropaolo^{9,10}, Craig J. Rodger²⁶, Trunali Shah²⁵,
14 Andy W. Smith²⁷, Nandita Srivastava²⁸, Bruce T. Tsurutani²⁹, S. Tulasi Ram²⁵, Lisa A. Upton³⁰,
15 Bhaskara Veenadhari²⁵, Sergio Vidal-Luengo³¹, Ari Viljanen¹⁹, Sarah K. Vines³, Vipin K.
16 Yadav³², Jeng-Hwa Yee¹⁴, James W. Weygand³³, and Eftyhia Zesta²
17

18 ¹ Goddard Planetary Heliophysics Institute, University of Maryland, Baltimore County, Baltimore, MD, USA

19 ² NASA Goddard Space Flight Center, Greenbelt, MD, USA

20 ³ Southwest Research Institute, San Antonio, TX, USA

21 ⁴ National Institute for Space Research, São José dos Campos, São Paulo, Brazil

22 ⁵ School of Physics, Trinity College Dublin, Merrion Square, Dublin, Ireland

23 ⁶ Dublin Institute for Advanced Studies, Dublin, Ireland

24 ⁷ SPACE Science Centre, School of Science, RMIT University, Melbourne, VIC, Australia

25 ⁸ Space and Atmospheric Science Division, Physical Research Laboratory Ahmedabad, Ahmedabad, India

26 ⁹ Department of Physical and Chemical Sciences, University of L'Aquila, Via Vetoio, 67100 L'Aquila, Italy

27 ¹⁰ National Institute of Astrophysics, IAPS, INAF-IAPS, 00133 Rome, Italy

28 ¹¹ Department of Physics, The Catholic University of America, Washington, DC, USA

29 ¹² Department of Physics and Astronomy, University of Iowa, Iowa City, IA, USA

30 ¹³ Department of Astronomy, University of Maryland, College Park, MD, USA

31 ¹⁴ Johns Hopkins University Applied Physics Laboratory, Laurel, MD, USA

32 ¹⁵ South African National Space Agency, Hospital Street, Hermanus P. O. Box 32, South Africa

33 ¹⁶ Space Science Institute, Boulder, CO, USA

34 ¹⁷ CAS Key Laboratory of Geospace Environment, School of Earth and Space Sciences, University of Science
35 and Technology of China, Hefei, People's Republic of China

36 ¹⁸ Institute for Space-Earth Environmental Research, Nagoya University, Nagoya, Aichi, Japan

37 ¹⁹ Finnish Meteorological Institute, Helsinki, Finland

38 ²⁰ Department of Physics and Technology, Birkeland Centre for Space Science, University of Bergen, Bergen,
39 Norway

40 ²¹ National Center for Atmospheric Research, Boulder, CO, USA

41 ²² Department of Climate and Space Sciences and Engineering, University of Michigan, Ann Arbor, MI, USA

42 ²³ Department of Physical Sciences, Indian Institute of Science Education and Research Kolkata, Mohanpur
43 741246, West Bengala, India

44 ²⁴ Center of Excellence in Space Sciences India, Indian Institute of Science Education and Research Kolkata,
45 Mohanpur 741246, West Bengala, India

46 ²⁵ Indian Institute of Geomagnetism, Navi Mumbai, India
47 ²⁶ Department of Physics, University of Otago, Dunedin, New Zealand
48 ²⁷ Department of Mathematics, Physics and Electrical Engineering, Northumbria University, Newcastle upon
49 Tyne, UK
50 ²⁸ Udaipur Solar Observatory, Physical Research Laboratory, Udaipur, India
51 ²⁹ Retired, Pasadena, CA, USA
52 ³⁰ Southwest Research Institute, Boulder, CO, USA
53 ³¹ Laboratory for Atmospheric and Space Physics, University of Colorado, Boulder, CO, USA
54 ³² Space Physics Laboratory (SPL), Vikram Sarabhai Space Centre (VSSC), Thumba, Thiruvananthapuram
55 695022, India
56 ³³ Department of Earth, Planetary and Space Sciences, University of California Los Angeles, Los Angeles, CA,
57 USA
58
59 * Correspondence: denny@umbc.edu
60

61 **Key points**

- 63 • Sunspot number and shock count data in SC23-24 are used with sunspot number
64 predictions for SC25 in a supervised regression model to estimate shock occurrence in
65 SC25
- 66
67 • Predictions indicate SC25 (275 events) will have ~48% more shocks in comparison to
68 SC24 (187 events), but it will have fewer shocks in comparison to SC23 (343 events)
69
- 70 • SC25 will offer unprecedented opportunities for space weather research given the
71 availability of many simultaneous data sets in the solar wind, geospace, and on the
72 ground
73

74 **Abstract**

75
76 Interplanetary (IP) shocks are perturbations observed in the solar wind. IP shocks correlate well
77 with solar activity, being more numerous during times of high sunspot numbers. Earth-bound IP
78 shocks cause many space weather effects that are promptly observed in geospace and on the
79 ground. Such effects can pose considerable threats to human assets in space and on the ground,
80 including satellites in the upper atmosphere and power infrastructure. Thus, it is of great interest
81 to the space weather community to 1) keep an accurate catalog of shocks observed near Earth,
82 and 2) be able to forecast shock occurrence as a function of the solar cycle (SC). In this work, we
83 use a supervised machine learning regression model to predict the number of shocks expected in
84 SC25 using three previously published sunspot predictions for the same cycle. We predict shock
85 counts to be around 275 ± 10 , which is ~47% higher than the shock occurrence in SC24 ($187 \pm$
86 8), but still smaller than the shock occurrence in SC23 (343 ± 12). With the perspective of
87 having more IP shocks on the horizon for SC25, we briefly discuss many opportunities in space
88 weather research for the remainder years of SC25. The next decade or so will bring

89 unprecedented opportunities for research and forecasting effects in the solar wind,
90 magnetosphere, ionosphere, and on the ground. As a result, we predict SC25 will offer excellent
91 opportunities for shock occurrences and data availability for conducting space weather research
92 and forecasting.

93
94

95 **Plain Language summary**

96

97 Solar activity is quite correlated with sunspot numbers. Alternating periods between solar
98 minima and maxima, termed solar cycle, usually occur every ~11 years. As a result, researchers
99 often attempt to predict sunspot occurrences for the following solar cycle. Solar perturbations
100 occur more frequently during periods of high solar activity, and Earth-bound perturbations can
101 disturb the Earth's magnetic field in geospace and on the ground, affecting satellites and power
102 infrastructure. In this work, we use an artificial intelligence supervised model to predict the
103 number of shock occurrences in the ongoing solar cycle (beginning December 2019) by training
104 the model with observations of sunspots and solar perturbations in the previous two solar cycles
105 (August 1996 to December 2019). Then, sunspot number predictions for the ongoing solar cycle
106 are applied to the model, and predictions for the solar perturbations are obtained. We find that
107 the number of predicted solar perturbations is ~50% higher than their occurrence number in the
108 previous solar cycle (December 2008 to December 2019). Finally, we discuss how this relatively
109 higher number of predicted solar perturbations can impact space weather research given the
110 unprecedented number of data sets available in geospace and on the ground in the upcoming
111 years.

112

113 **1. Introduction**

114

115 Interplanetary (IP) shocks are solar wind structures observed in the heliosphere ([Kennel et al., 1985](#);
116 [Echer et al., 2003](#); [Tsurutani et al., 2011](#)). As IP shocks strike Earth, they cause
117 perturbations frequently observed in geospace and on the ground, with significant implications
118 for space weather. In geospace, IP shocks accelerate particles associated with solar energetic
119 particle events ([Tsurutani & Lin, 1985](#); [Reames, 1999](#); [Malandraki & Crosby, 2017](#)); affect
120 radiation belt dynamics ([Kanekal et al., 2016](#), [Baker et al., 2018](#)); enhance field-aligned currents
121 ([Kasran et al., 2019](#); [Shi et al., 2019](#)); trigger ultra-low frequency (ULF) waves in the
122 magnetosphere-ionosphere (MI) system ([Zong et al., 2009](#); [Hartering et al., 2022](#)); trigger
123 magnetospheric substorms ([Akasofu & Chao, 1980](#); [Zhou & Tsurutani, 2001](#)); and intensify
124 ionospheric total electron content (TEC) ([Tulasi Ram et al., 2019](#); [Chen et al., 2023](#)).

125

126 On the ground, IP shocks cause positive magnetic sudden impulses (SI⁺) detected by low- and
127 mid-latitude stations ([Araki, 1977](#); [Andrioli et al., 2006](#); [Villante & Piersanti, 2011](#)), and
128 generate ground magnetic field variations that cause geomagnetically induced currents (GICs)
129 ([Carter et al., 2015](#); [Oliveira & Ngwira, 2017](#)), which can impact power transmission lines and
130 infrastructure ([Oughton et al., 2017](#)). Therefore, keeping an updated and accurate IP shock data

131 base with events observed upstream of the Earth at the Lagrangian L1 point is of paramount
132 importance to the space weather community (Oliveira, 2023a).

133
134 IP shocks are frequently driven by solar wind perturbations termed coronal mass ejections
135 (CMEs) (Bame et al., 1979; Gosling, 1997), and corotating interaction regions (CIRs) (Smith &
136 Wolfe, 1976; Jian et al., 2006). For Earth-bound shocks observed at L1, CME-driven shocks
137 usually have their shock normal vectors aligned with the Sun-Earth line (e.g., Byrne et al., 2010),
138 whereas CIR-driven shocks usually have their shock normal vectors with large inclinations with
139 respect to the Sun-Earth line following the Parker spiral structure (e.g., Balogh et al., 1999).
140 Nearly frontal shock impacts usually trigger larger geomagnetic activity at Earth in comparison
141 to highly inclined shocks due to highly symmetric magnetospheric compressions and the
142 subsequent effective enhancements of the MI current systems in the former case (Oliveira &
143 Samsonov, 2018; Oliveira, 2023b). Most of the phenomena discussed in this paper are also
144 caused by sheaths and magnetic structures (clouds) following CMEs (Kilpua et al., 2019) and
145 further compression effects by CIRs (Richardson et al., 2006), but our focus is on compression
146 effects caused by shocks.

147
148 The Sun is an active star with a magnetic cycle which involves both amplitude modulation and
149 polarity reversal in its magnetic field. The reversal of its magnetic field polarities occurs every
150 ~11 years taking ~22-years on the average for a complete magnetic cycle which is known as the
151 Hale cycle (Hale & Nicholson, 1925). Consequently, the Sun presents a cyclic modulation of
152 sunspot number observations corresponding to ~11 years, which will be referred to as the solar
153 cycle (SC) in this work (Hathaway, 2015). Solar activity cycle is produced by a
154 magnetohydrodynamic dynamo mechanism working in its interior which involves interactions
155 between plasma flows and fields (Hazra et al., 2023). Physical models and empirical techniques
156 have been used with varying degrees of success in predicting the sunspot cycle amplitude
157 (Bhowmik & Nandy 2018, Bhowmik et al., 2023) with a consensus emerging that SC25 is going
158 to be a weak-moderate cycle slightly stronger than SC24 in terms of low sunspot numbers
159 (Nandy, 2021). The dynamo produced magnetic fields emerge as sunspots through the Sun's
160 surface giving rise to a plethora of activity, including energetic events that have space weather
161 consequences thereby connecting variations that originate in the Sun to near-Earth space (Nandy
162 et al., 2021, 2023).

163
164 At Earth, high geomagnetic activity usually occurs during periods of numerous sunspot
165 observations (Hathaway, 2015; Vázquez et al., 2016; Chapman et al., 2020). Even though
166 humanity has been observing sunspots by telescopes for four centuries (Stephenson, 1990;
167 Vaquero & Vázquez, 2009), current solar cycle predictions can be quite challenging, frequently
168 disagreeing with one another (Pesnell, 2015; Nandy, 2021). More important to our current work,
169 IP shock occurrences are strongly correlated with sunspot observations, being more numerous
170 during periods of solar maxima (Oh et al., 2007; Kilpua et al., 2015; Oliveira & Raeder, 2015).
171 CME-driven shocks tend to follow the solar cycle, but CIR-driven shocks occur more often
172 during descending phases of the solar cycle without clear correlations with sunspot numbers

173 (e.g., Borovsky & Denton, 2006; Kilpua et al., 2015). Therefore, highly geoeffective and nearly
174 frontal shocks tend to be more numerous during solar maxima (Oliveira, 2023a). Multi-solar-
175 cycle analyses have shown that 3 out of 4 IP shocks are followed by magnetic storms with
176 significant levels of geomagnetic activity (E.J. Smith et al., 1986; Wang et al., 2006; Mansilla,
177 2014; Fogg et al., 2023). Therefore, being able to predict IP shock occurrence as a function of
178 solar cycle is clearly a very useful space weather forecasting tool (A.W. Smith et al., 2020).

179
180 In this work, we use the IP shock catalog provided by Oliveira (2023a) and sunspot number
181 observations, along with previously published sunspot number predictions for SC25, to predict
182 shock number occurrences for SC25. By using a supervised machine learning regression model,
183 we estimate the number of shocks in SC25 to be higher than the occurrence in the notoriously
184 weak SC24, but we find that SC25 will have fewer shocks in comparison to SC23. Moving
185 forward, we briefly discuss the many opportunities for space weather research in the following
186 years. Particularly in the ongoing solar cycle there are and there will be enhanced levels of
187 simultaneous data sets collected in the solar wind, magnetosphere, ionosphere, and on the
188 ground. One expects this period will provide unprecedented measurement numbers since the
189 advent of the space era. As follows, Section 2 describes the data used in this article. Section 3
190 presents the prediction results. Section 4 briefly summarizes the main MI current systems
191 affected by SI^+ events caused by shock compressions. Section 5 briefly discusses many topics
192 with opportunities for space weather research, including possibilities of multipoint observations
193 throughout the MI system and on the ground. Finally, Section 6 concludes the paper.

194 195 **2. Data**

196
197 In this work, we use the IP shock catalog provided by Oliveira (2023a) with 618 events from
198 January 1995 to December 2023. The list covers nearly three decades of solar wind observations
199 by Wind (Harten & Clark, 1995), Advanced Composition Explorer (ACE) (Stone et al., 1998),
200 and Deep Space Climate Observatory (DSCOVR, a replacement to ACE) (Loto'aniu et al.,
201 2022). The authors then celebrate nearly 30 years of observations from Wind, which accounts for
202 55% of the shock observations in the list as part of many other discoveries in astrophysics and
203 heliophysics (Wilson III et al., 2021). The current list evolved from previous lists published by
204 Oliveira and Raeder (2015), Oliveira et al. (2018), and Wang et al. (2010), along with online
205 catalogs of shocks detected with Wind and ACE data located at
206 http://www.cfa.harvard.edu/shocks/wi_data/ and http://www-ssg.sr.unh.edu/mag/ace/ACELists/obs_list.html#shocks. The methodologies used to identify the
207 shocks and calculate their properties, including data processing, are explained in detail by
208 Oliveira (2023a).

209
210
211 The other primary data set used in this work are the sunspot number (SSN) observations
212 provided by the World Data Center for Geomagnetism, Kyoto et al. (2015), and Long-term Solar
213 Observations (WDC-SILSO), from the Royal Observatory of Belgium. The SSN catalog,
214 spanning over three centuries, was revised by Clette et al. (2023), who recalibrated the data by

215 updating previous scaling factors and introducing common symbols representing the data. The
216 SSN data set is explained by [Clette et al. \(2023\)](#) and routinely updated by SILSO.

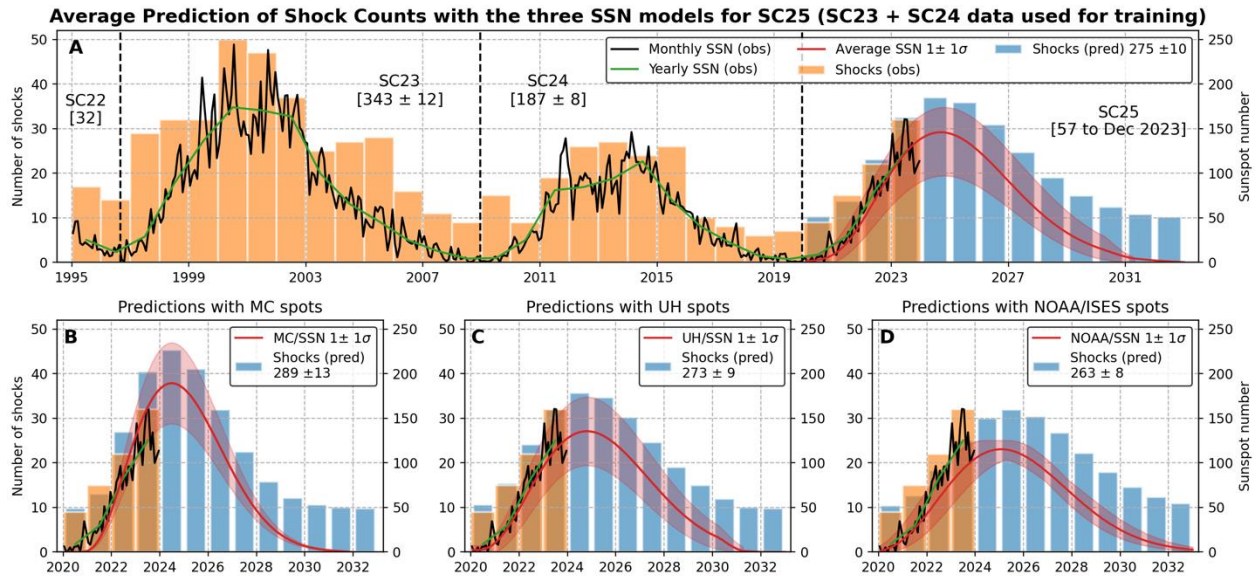
217
218 Monthly sunspot number data predictions for SC25 are provided by three different sources. The
219 first sunspot predictions were performed by [McIntosh et al. \(2023\)](#), who used in their study the
220 transition of the Hale Cycle terminator that marks the SC24-25 transition in the Sun's Hale cycle
221 ([McIntosh et al., 2020](#)). Second, we use sunspot prediction data published by [Upton and
222 Hathaway \(2023\)](#). Those authors used curve fitting methods applied to the first 3-4 years of
223 sunspot observations in SC25, which was already under way in their analysis. Finally, the third
224 sunspot prediction data set is provided by a panel formed by three different organizations,
225 namely NASA, NOAA, and ISES (International Space Environment Service,
226 <https://www.swpc.noaa.gov/products/solar-cycle-progression>). Henceforth, these data sets will
227 be referred to as the monthly MC, UH, and NOAA predicted sunspot number data, respectively.
228

229 **3. Shock number predictions for solar cycle 25**

230
231 Shock count predictions for SC25 are obtained with a supervised regression analysis method
232 commonly used in machine learning investigations (e.g., [Rong & Bao-wen, 2018](#)). This method
233 involves applying a nonlinear function f to an N-dimensional list of observations x to obtain
234 predictions of y such as $y = f(x) + \varepsilon$, where ε is a stochastic error or noise term ([Bishop, 2016](#);
235 [Camporeale, 2019](#)). In this work, we specifically use the Python *scikit-learn*¹ package
236 (*LinearRegression* function of the *linear_model* module), which reduces errors with the least
237 square method by minimizing the sum of the squares of the residuals ([Pedregosa et al., 2011](#)).
238 Supervised linear regression functions are commonly used in space weather investigations, e.g.,
239 solar flare forecasting ([Benvenuto et al., 2018](#)), predictions of several ionospheric parameters
240 including electron density and TEC ([Sai Gowtam et al., 2019](#); [Iban & Şentürk, 2022](#)), predictions
241 of storm sudden commencement occurrence following IP shocks ([A.W. Smith et al., 2020](#)), and
242 predictions of thermospheric neutral mass density ([Licata & Mehta, 2022](#)). Since (on average)
243 sunspot number predictions for SC25 are in between the observed sunspot numbers of SC23 and
244 SC24, we choose the previous two solar cycles for training the model. After training, fitted
245 coefficients are applied to the model along with yearly-averaged SSN predictions (MC, UH, and
246 NOAA) for SC25 to obtain shock count predictions for the same solar cycle.

247

¹ https://scikit-learn.org/stable/modules/classes.html#module-sklearn.linear_model



248
 249 *Figure 1. All panels: observed SILSO sunspot number (SSN, monthly, black; yearly, green) data; yearly shock counts from the*
 250 *data base provided by Oliveira (2023a) (faint orange bars). These data are represented from 1995 to 2023 (panel A), and from*
 251 *2020-2032 (panels B-D). In all panels, predictions of shock counts (faint blue bars) for solar cycle 25 were obtained with*
 252 *sunspot number predictions provided by McIntosh et al. (2023) (MC, panel B); Upton and Hathaway (2023) (UH, panel C); and*
 253 *NOAA (panel D). The thick red lines indicate monthly sunspot number predictions obtained from the respective source (the*
 254 *highlighted red regions indicate $\pm 1\sigma$ estimations). Faint blue bars in panel A show the average shock number predictions for*
 255 *solar cycle 25, whereas the thick red line indicates the mean sunspot number value obtained from the three sources.*

256 In all panels of Figure 1, the solid black and green lines represent, respectively, SSN monthly
 257 and yearly observations, and the orange bars indicate yearly shock counts from the Oliveira
 258 (2023a) catalog. Panel A shows data from January 1995 to December 2023, whereas panels B-D
 259 show data from January 2020 to December 2023. The vertical dashed black lines indicate the
 260 limits from the end of SC22 to the beginning of SC25. The thick red lines indicate the MC
 261 sunspot number predictions (panel B); the UH sunspot number predictions (panel C); and the
 262 NOAA sunspot number predictions (panel D). The highlighted areas in these panels indicate $\pm 1\sigma$
 263 estimations for the corresponding sunspot number prediction. The same in panel A indicates the
 264 mean sunspot number predictions obtained from the predicted data shown in panels B-D (thick
 265 red lines). The SC25 shock count predictions are represented by the light blue bars in panel B
 266 obtained from MC sunspot data; panel C, UH sunspot data; and panel D, NOAA sunspot data.
 267 The light blue bars in panel A indicate the mean of the three shock count predictions for SC25.
 268 The maximum monthly sunspot predictions by the models are: 184 ± 17 (MC), 134 ± 8 (UH),
 269 and 115 ± 6 (NOAA), and the average is 144 ± 10 . Note this comparison is summarized in Table
 270 1. The Supporting Information brings results obtained from similar analysis when SC23 and
 271 SC24 SSN and shock occurrence data are used for training, as well as further validations with
 272 historical F10.7 solar flux index data (1964 to 2023).

273
 274
 275
 276
 277
 278

279 *Table 1 Summary and comparison of the statistical results obtained for observations (SC23 and SC24) and predictions (SC25)*
 280 *for sunspot numbers (white rows) and shock occurrences (grey rows), respectively. MC represents the McIntosh et al. (2023)*
 281 *predictions; UH, Upton and Hathaway (2023) predictions; and the NOAA predictions. In the rightmost column, observation*
 282 *values are shown in normal text (SC23 and SC24), whereas the predicted mean values are shown in bold text (SC25).*

	MC (# \pm 1 σ)	UH (# \pm 1 σ)	NOAA (# \pm 1 σ)	Obs./Pred. (# \pm 1 σ)
Max Sunspots SC23	-	-	-	244 \pm 10
Shocks SC23	-	-	-	343 \pm 12
Max Sunspots SC24	-	-	-	146 \pm 6
Shocks SC24	-	-	-	187 \pm 8
Max Sunspots SC25	184 \pm 17	134 \pm 8	115 \pm 6	144 \pm 10
Shocks SC25	289 \pm 13	273 \pm 9	263 \pm 8	276 \pm 10

283
 284 The MC shock count predictions are the highest (289 \pm 13) because the MC sunspot predictions
 285 are the highest. Moderate shock count predictions are obtained with UH sunspots (273 \pm 9),
 286 whereas the lowest shock predictions are obtained with NOAA sunspots (263 \pm 8). Therefore,
 287 shock counts are predicted to be ~40%-55% higher than the shock number occurrence in SC24
 288 (Table 1), being on average ~47% higher. Thus, regardless of the sunspot prediction data used,
 289 the numbers of shocks occurring in SC25 are predicted to be higher in comparison to SC24 (187
 290 \pm 8), but lower in comparison to SC23 (343 \pm 12). Additionally, our predictions indicate that the
 291 number of shocks in SC25 will be closer to the number of shocks in SC23 in comparison to the
 292 number of shocks in SC24 (Table 1). These results differ from the conclusions of Gopalswamy et
 293 al. (2023), who predicted that the number of CMEs observed in SC25 will also be in between the
 294 CME observation numbers of SC23 and SC24, but closer to the lower limit (i.e., SC24). Our
 295 predictions also indicate a larger number of shocks occurring during the declining phase of
 296 SC25, in agreement with SC23. Such shocks may most likely be driven by CIRs (Kilpua et al.,
 297 2015), which are not accounted for in Gopalswamy et al. (2023)’s analysis.

298
 299 As shown in Figure 1A, after 2020, the average sunspot number prediction (thick red line) agrees
 300 well with sunspot observations being performed until December 2023 (monthly and yearly
 301 observations). These comparisons bring confidence to our results, as can be clearly seen in the
 302 remarkable agreement between the number of observed (78) and (average) predicted (80) shocks
 303 from 2020 to 2023 (faded orange and blue bars, respectively).

304
 305 The number of shocks predicted for SC25 are expected to be observed at low heliospheric
 306 distances, namely the Lagrangian L1 point. Based on the knowledge of shocks observed at 1 AU,
 307 we expect that the shocks observed in SC25 will mostly be driven by CMEs in comparison to
 308 CIRs (Kilpua et al., 2015). We expect this to be the case because CIR-driven shocks are more
 309 likely to be observed farther in the heliosphere, beyond 3-5 AU (Smith & Wolfe, 1976;
 310 Richardson, 2018). Additionally, the predicted CME-driven shocks are expected to be stronger
 311 than the CIR-driven shocks in SC25 (Kilpua et al., 2015).

312
 313

314 **4. MI current response to SI⁺ events at different latitudes and longitudes**

315

316 The first MI current promptly affected by IP shock impacts is the dayside magnetopause current,
317 located at distances > 10 Earth radii from the ground (Chapman & Ferraro, 1931; Cahill &
318 Amazeen, 1963). During SI⁺ events, the horizontal component of the geomagnetic field increases
319 at different latitudes due to changes in the magnetopause current associated with the dayside
320 compression of the magnetosphere (Burton et al., 1975; Russell et al., 1994; Fiori et al., 2014).
321 Additionally, there exist two ionospheric current systems around 100 km altitude that are usually
322 associated with more latitudinally-localized geomagnetic perturbations that are significantly
323 enhanced by shocks. Such currents are located at auroral regions, namely the auroral electrojet
324 current, which is intensified by enhancements of the Region 1 current (Araki, 1977; Cowley,
325 2000). The other ionospheric current system affected by shocks is located at a region centered at
326 $\pm 3^\circ$ from the dip magnetic equator. This region carries an electric current named the equatorial
327 electrojet current, which shows strong diurnal variations, with maxima typically observed during
328 the early afternoon sector (Forbes, 1981; Lürh et al., 2004). The equatorial electrojet current is
329 directly proportional to the Cowling conductivity through electron densities and the zonal
330 electric field (Cowley, 2000; Kelley, 2009).

331

332 During SI⁺ events, the sudden compressions of the current systems described above cause
333 prompt variations of the horizontal component of the geomagnetic field, namely ground dB/dt
334 variations. These geomagnetic perturbations are linked through Faraday's law ($\text{curl } \mathbf{E} = -d\mathbf{B}/dt$)
335 to GICs (Viljanen, 1998; Boteler & Pirjola, 2017). Although dB/dt is commonly accepted as one
336 of the most important space weather drivers of, and are frequently used as a metric for, GICs
337 (Pulkkinen et al., 2017; Dimmock et al., 2020), actual GICs show spectral dependence of dB/dt
338 variations due to their coupling with the three-dimensional solid Earth conductivity (Oliveira &
339 Ngwira, 2017; Liu et al., 2019; Kelbert & Lucas, 2020; Juusola et al., 2020). Auroral dynamics
340 is also an important space weather driver of GIC effects at high latitudes (Tsurutani & Hajra,
341 2023; Wawrzaszek et al., 2023). GICs can cause detrimental effects to many ground artificial
342 conductors such as power transmission lines and infrastructure (Gaunt & Coetzee, 2007;
343 Pulkkinen et al., 2017), oil/gas pipelines (Campbel, 1980; Gummow & Eng, 2002), railways
344 (Thaduri et al., 2020; Patterson et al., 2023), and even submarine cables (Chakraborty et al.,
345 2022; Boteler et al., 2024). Historical data also show that GICs caused significant damage to old
346 telegraph wires during intense auroral activity events (Barlow, 1849; Arcimis, 1903; Silverman,
347 1995; Hayakawa et al., 2020a). Therefore, identifying current systems that cause GICs and being
348 able to predict solar wind drivers (including IP shocks) that intensify currents in the MI system is
349 of paramount importance to space weather applications and forecasting.

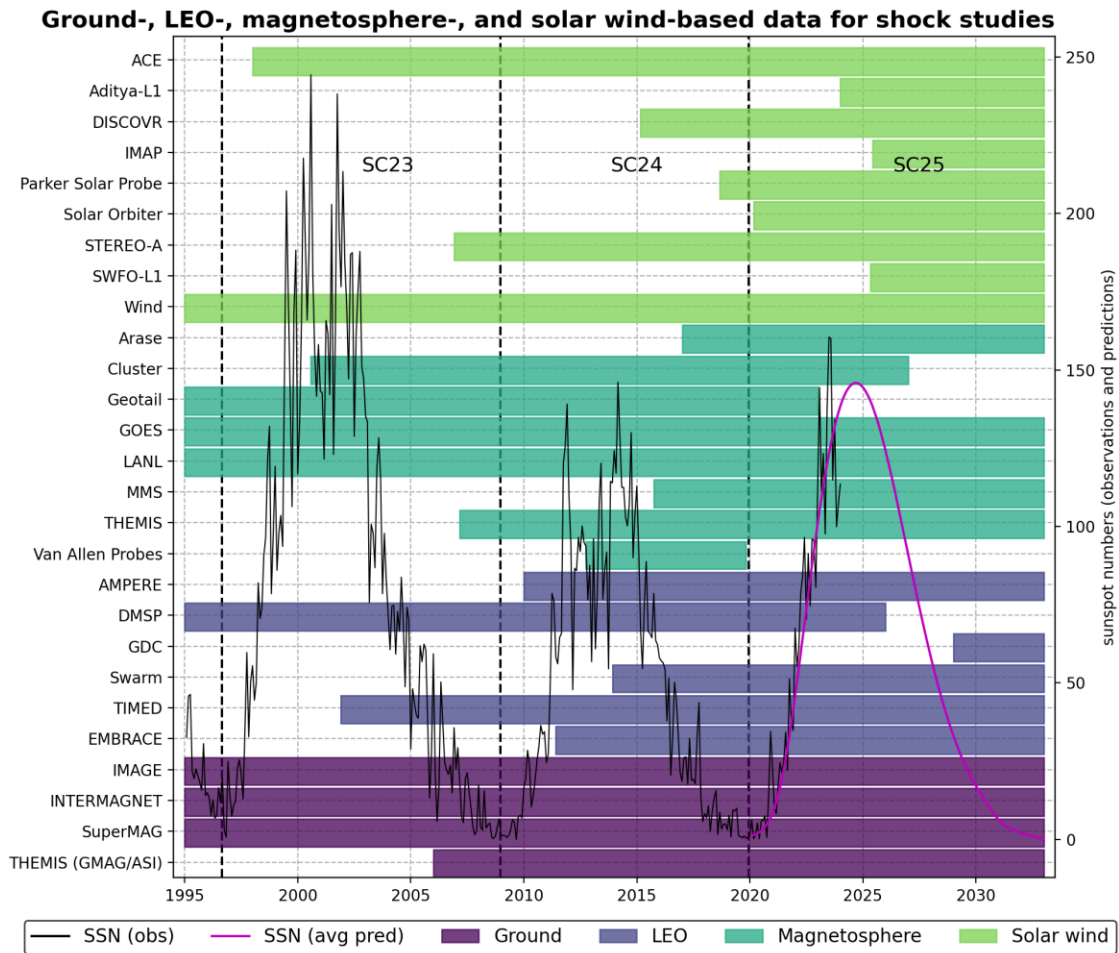
350

351 The geomagnetic field is often approximated to a geocentric dipole field in many regions of the
352 magnetosphere (Laundal & Richmond, 2017). However, as shown by observations (Pavón-
353 Carrasco & De Santis, 2016) and modeling (Finlay et al., 2020; Alken et al., 2021) of the Earth's
354 magnetic field, there is a region where the geomagnetic field is notably weaker in comparison to
355 the dipole field. This region is known as the South Atlantic Anomaly (SAA) region, which has

356 been moving from South Africa to South America at a mean rate of $0.17^\circ/\text{year}$ (westward) and
 357 $0.03^\circ/\text{year}$ (southward) in the past four centuries (Hartmann & Pacca, 2009). The radiation belts
 358 within SAA reach the lowest altitudes (Vernov et al., 1967; Gledhil, 1976; Heitzler, 2002). For
 359 this reason, the SAA is a region where intense energetic particle fluxes (H.S. Zhao et al., 2020;
 360 Kovář & Sommer, 2021) can pose serious threats to satellites that fly through it (Vernov et al.,
 361 1967; Heitzler et al., 2002; Schaeffer et al., 2016; Kovář & Sommer, 2021). However, recent
 362 research performed by Liu et al. (2024) with auroral intensity observations indicates that the
 363 weakened magnetic field in the SAA subsequently weakens the corresponding longitudinal
 364 extension of the auroral structure in the SAA. This effect is not observed in the northern
 365 hemisphere. Auroral and equatorial electrojets in the SAA may contribute to ground dB/dt
 366 variations associated with GICs on the ground in the corresponding latitudes and longitudes.

367
 368 In the next section we discuss how past, current, and future data sets in the solar wind, geospace,
 369 and on the ground can be used to investigate the response of the current systems discussed above
 370 to shocks. The focus is on how the predicted higher number of shocks in SC25 in comparison to
 371 SC24 may provide some new opportunities of research in the solar wind, magnetosphere,
 372 ionosphere, and on the ground.

373



374
 375

376 *Figure 2. Chronological durations of operation and commission times for 25 ground magnetometer arrays and satellite missions*
377 *whose data can be used in interplanetary shock and space weather research. Satellite missions shown in the plot*
378 *operate/operated in low-Earth orbit (ionosphere and thermosphere), in the magnetosphere and solar wind (see legend). The*
379 *black dashed vertical lines mark the end of SC22 to the beginning of SC25. By the end of SC25, there will be more than 20 data*
380 *sets available for shock and space weather research on the ground and in space as never seen in six decades of shock studies*
381 *since the first observations of collisionless shocks in the solar wind in early 1960's (Oliveira and Samsonov, 2018). The solid*
382 *black and magenta lines on top of the bars indicate sunspot observations (January 1995 to December 2023) and mean sunspot*
383 *predictions (January 2020 to December 2032).*

384

385 **5. Discussion**

386

387 Here, we briefly discuss how an increased number of shocks (and possibly stronger events)
388 observed at L1 can contribute to space weather research in different regions of the heliosphere
389 (solar wind, magnetosphere, ionosphere, and ground). We also highlight the importance of multi-
390 instrument studies concerning geomagnetic activity triggered by shocks considering the multi-
391 data set availability for SC25, as shown in Figure 2. The figure shows commission times of
392 satellites (solar wind, magnetosphere, ionosphere) and time spans of ground magnetometer
393 deployments for many data sets during the time span of the shock catalog (Oliveira, 2023a)
394 including the rising phase of SC25 (observations) and predictions. Some of these missions and
395 ground data will be discussed with some detail below. In the discussion, except for missions that
396 have already ended (Geotail and Van Allen Probes), and missions that are scheduled to be
397 decommissioned in the following years (Cluster and DMSP), all missions are assumed to be
398 carrying on their observations throughout SC25.

399

400 **5.1 Solar wind**

401

402 As a highlight mission featuring in this work, Aditya-L1, launched by the Indian Space Agency
403 and already operational, is the first Indian mission to study the Sun (Somasundaran & Megala,
404 2017; Tripathi et al., 2023). Aditya-L1 carries two in-situ experiments, the charged particle
405 detectors for measuring the solar wind (ions and electrons) and energetic particles (primarily
406 protons and alpha particles), described by Goyal et al. (2018), and one for interplanetary
407 magnetic field (IMF) measurements, described by Yadav et al. (2018). Some of the main goals of
408 Aditya-L1 are to study the physics of the solar corona and its heating mechanism; the origin,
409 development, and dynamics of CMEs; understand the origin and acceleration mechanism of solar
410 wind and energetic particles in the solar wind; and detect/characterize space weather drivers,
411 including IP shocks.

412 NOAA's Space Weather Follow-On (SWFO) mission at L1 (SWFO-L1) will also monitor the
413 solar wind (Vargas et al., 2024). By gathering real-time data at the L1 point, NOAA aims to
414 improve the accuracy and timeliness of space weather forecasts. The SWFO-L1 instruments are
415 expected to be part of the broader SWFO mission, including observations in geostationary orbits
416 by Geostationary Operational Environmental Satellite - Series U (GOES-U), which was planned
417 for launch in 2024 (Vargas et al., 2024). The deployment at the L1 point signifies NOAA's
418 commitment to advancing space weather forecasting capabilities, leveraging strategic positioning
419 to gather critical data about solar activity before it impacts Earth's space environment.

420 NASA's Interstellar Mapping and Acceleration Probe (IMAP) mission is designed to investigate
421 the boundary between our solar system and interstellar space (McComas et al., 2018). IMAP's
422 primary objective is to study the heliosphere. Specifically, IMAP aims to understand the
423 interactions between the solar wind and the interstellar medium as well as the dynamics of
424 cosmic rays. IMAP is planned to be launched aboard a SpaceX Falcon 9 rocket in 2024. Since
425 IMAP will also be placed in a highly elliptical orbit around the Sun-Earth L1 point, it will
426 provide measurements of solar wind properties and IMF as well.

427 Aditya-L1, SWFO-L1, and IMAP solar wind plasma parameter and IMF data will significantly
428 contribute to the maintenance of the IP shock catalog maintained by Oliveira (2023a). Those
429 spacecraft will join Wind and DSCOVR in providing data for shock identification and
430 computation of shock properties. The missions join L1 at an important time because the Wind
431 instruments, though still operational, are aging², and our predictions indicate more shocks will hit
432 L1 in SC25 in comparison to SC24; therefore, having stable solar wind monitors at L1 is of
433 paramount importance to space weather research, as well as predicting and forecasting solar
434 wind events. In addition to Wind, DSCOVR, Aditya-L1, SWFO-L1, and IMAP at L1, Solar
435 Orbiter (Müller et al., 2020), and STEREO (Solar Terrestrial Relations Observatory) (Kaiser,
436 2005) will be used for combined observations to compute shock properties in SC25. For
437 example, Laker et al. (2024) used combined Solar Orbiter and STEREO observations to predict
438 the arrival at Earth of a CME with high accuracy.

439
440 IP shocks also play a crucial role in CME-CME interaction. If a shock from the leading CME
441 penetrates the preceding CME, it provides a unique opportunity to study the evolution of the
442 shock strength and structure and its effects on preceding CME plasma parameters (Lugaz et al.,
443 2005; Möstl et al., 2012; Liu et al., 2012). For instance, Wang et al. (2003) showed that an IP
444 shock can cause an intense southward magnetic field of long duration in the preceding magnetic
445 cloud, which is crucial for space weather predictions (Jurac et al., 2002). Srivastava et al. (2018)
446 reported a case of interacting CMEs observed on 13-14 June 2012 in which the shock of the
447 following CME led to a strong SI^+ (~150 nT) with a long duration rise time of 20 hrs. Mishra et
448 al. (2021) suggested that the structures associated with interacting CMEs, possibly resulting from
449 large-scale deflections, may arrive at larger longitudinally separated locations in the heliosphere.
450 Multipoint in situ analyses highlighted that the characteristics of the same shock, propagating in
451 a pre-conditioned medium, can be different at distinct longitudinal locations in the heliosphere
452 (Kilpua et al., 2011). Thus, enhanced observations of IP shocks in SC25 and many solar wind
453 monitors (Figure 2) will provide a unique opportunity with multi-point observations to study IP
454 shocks that arrive at different locations in the heliosphere, including L1.

455
456 Accurately estimating the occurrence rate of IP shocks during different solar cycle phases is
457 important for heliophysics space mission design. For example, a major goal of the Solar WInd
458 Multi-Scale (SWIMS) mission, previously known as Seven Sisters (Nykyri et al., 2023), is to
459 determine the intermediate and large-scale structure of the solar wind. For the first time, SWIMS
460 will be able to determine simultaneously the radial evolution and azimuthal structure of CMEs,
461 as well as capture the multi-scale properties of the heliospheric current sheet (Ness & Wilcox,

² <https://spacenews.com/noaa-warns-of-risks-from-relying-on-aging-space-weather-missions/>

462 [1964; E.J. Smith et al., 1978; Tsurutani et al., 1995](#)), stream interaction regions and determine
463 the physical processes responsible for particle acceleration in these structures. The present
464 machine learning IP shock prediction tool can be used to achieve a more accurate estimate of the
465 amount of shock crossings during different mission phases. This is necessary to estimate the
466 volume requirements for the burst mode data, design on-board data storage, and plan
467 communications and downlinking schedule.

468
469 The Lunar Gateway is a space station scheduled to orbit the Moon in a Near Rectilinear Halo
470 Orbit (NRHO) by the end of 2025 ([Fuller et al., 2022](#)). As a multi-international agency endeavor,
471 Gateway is a key part of NASA's Artemis program, which aims to establish human presence on
472 the Moon. Moreover, Gateway will serve as a space port to facilitate future lunar and Mars
473 missions and deep space exploration ([M. Smith et al., 2020](#)). HERMES (Heliophysics
474 Environmental and Radiation Measurement Experiment Suite) is the space weather instrument
475 suite that will be continuously monitoring the lunar space environment on Gateway ([Paterson et
476 al., 2021](#)). HERMES will support the Artemis program by providing space weather observations
477 of the Earth's magnetospheric variabilities and solar wind interactions with the Moon. For
478 example, [Omidi et al. \(2023\)](#) have demonstrated with observations and simulations that IP
479 shocks significantly impact local density and accelerate energetic ions in the lunar tail. Since
480 these shocks may affect the objectives of the Artemis project, it is important to be able to predict
481 shock occurrences in SC25, even though shocks observed at lunar distances are weaker in
482 comparison to shocks observed at L1 ([Halekas et al., 2014](#)). Moreover, the assessment of space
483 weather phenomena is clearly highly relevant for sustainable lunar exploration activities
484 ([Fogtman et al., 2023](#)) but are also required for future missions to Mars ([Green et al., 2022](#)).
485 Therefore, our predictions indicate that a higher number of shocks in SC25 can generate an
486 impact on the Artemis program objectives and on future deep space exploration missions.

487 488 **5.2 Magnetosphere**

489
490 [Oliveira et al. \(2020\)](#) and [Oliveira et al. \(2021\)](#) have used Magnetospheric Multiscale (MMS)
491 magnetic field data to compute the average propagation direction of compression waves induced
492 by shock impacts with different orientations on the magnetosphere. The authors demonstrated
493 that the propagation direction of the compression waves is quite aligned with the propagation
494 direction of the inducing shock impacting the magnetosphere ([Collier et al., 2007](#)). [Oliveira et al.
495 \(2020\)](#) and [Oliveira et al. \(2021\)](#) used this supporting information provided by MMS
496 observations in the magnetosphere to show that the subsequent geomagnetic activity following
497 the shocks (e.g., ULF wave activity and ground dB/dt variations) were indeed triggered under
498 very asymmetric magnetospheric compression states.

499
500 However, a statistical follow-on investigation to probe the conclusions of [Oliveira et al. \(2020\)](#)
501 and [Oliveira et al. \(2021\)](#) is difficult to be undertaken with current data due to two reasons: first,
502 MMS was launched during the declining phase of SC24 (September 2015), and second, SC24
503 was one of the weakest solar cycles since the Dalton Minimum ([Figure 1A; see also Hayakawa et](#)

504 [al., 2020b; Clette et al., 2023](#)). Therefore, with an increased number of shocks in SC25, such a
505 statistical analysis should be possible, eventually including magnetopause crossings observed by
506 MMS ([Dong et al., 2018; Oliveira et al., 2020; 2021](#)). A statistical picture of the two-dimensional
507 structure of current sheets associated with partial magnetopause crossings performed by MMS
508 ([Dong et al., 2018](#)) may also be possible.

509
510 As mentioned in the introductory section, IP shocks are known to accelerate charged particles
511 across its surface. Additionally, IP shocks can inject energetic electrons in the magnetosphere
512 very rapidly, within a time scale of a few minutes or a few electron drifts ([Blake et al., 1992;](#)
513 [Baker et al., 2018; Kanekal & Miyoshi, 2021](#)). Such energetic particles play a significant role in
514 affecting the chemistry of the upper atmosphere with further space weather implications
515 ([Turunen et al., 2016](#)). Although the Van Allen Probes were a successful mission to study the
516 radiation belts ([Mauk et al., 2014](#)), Van Allen Probes operated during the relatively weak SC24
517 period when only ~120 shocks were observed at L1 ([Oliveira, 2023a](#)). Despite this, [Schiller et al.](#)
518 ([2016](#)) were able to carry out a statistical analysis of IP shock effects on the subsequent energy
519 of the injected electrons observed by Van Allen Probes and found that the highest energetic
520 electrons occurred as a response to the strongest shocks. These results suggest that IP shocks
521 most likely control energetic electron injections since the strongest shocks tend to be the most
522 nearly frontal shocks ([Oliveira et al., 2018](#)). Therefore, three questions are still open: how do
523 shock impact angles 1) affect the time duration of energetic electron injections into the
524 magnetosphere; 2) control energetic electron injections as a function of L-shell; and 3) control
525 the intensity of the energetic electron injections into the magnetosphere? In contrast, the
526 exploration of Energization and Radiation in Geospace (ERG) mission, better known as Arase, a
527 Japanese mission to study the radiation belt environment, was launched in 2017 and is still
528 healthy ([Nakamura et al., 2018; Miyoshi et al., 2022](#)). Although some conjugate observations
529 with Van Allen Probes and Arase data were conducted ([Miyoshi et al., 2022](#)), Arase will be able
530 to study energetic particle injections as a function of shock impact angles with a more robust
531 statistical sample including more and stronger shocks than the events observed by Van Allen
532 Probes in SC24. Because Arase performs observations at higher L-shells in comparison to Van
533 Allen Probes ([Miyoshi et al., 2022](#)), Arase will be able to sample energetic particle injections in
534 a larger array of L-shells in comparison to Van Allen Probes.

535
536 IP shocks can also significantly impact energetic ion compositions (H^+ , O^+ , and He^+) within the
537 Earth's magnetosphere. For example, [Yue et al. \(2016\)](#) investigated, with Van Allen Probes data
538 when the satellites were near the equator, the increase in low-energy ions (<100 eV) associated
539 with field enhancements caused by shocks and the related ULF wave activity. Also, observations
540 at high latitudes have shown that sharp and sudden changes in the solar wind dynamic pressure
541 associated with IP shocks can enhance ion outflow (e.g., [Fuselier et al., 2001; Moore et al.,](#)
542 [1999](#)). Ionospheric outflowing ions are one of the two sources of ions in the Earth's
543 magnetosphere ([Kistler et al., 2023, and references therein](#)). Ion outflow can come from different
544 latitudes in the ionosphere and populate different regions in the magnetosphere. For example, at
545 high latitudes, in the domain of open field lines, outflowing ions can reach the lobes, mantle, and

546 cusp (e.g., [K. Zhao et al., 2020](#)), and at lower latitudes, in the domain of closed field lines, they
547 reach the plasma sheet and the inner magnetosphere (e.g., [Gkioulidou et al., 2019](#)). Outflowing
548 ions often have thermal energies up to a few eV, but more energetic ion outflows with energies
549 of tens to hundreds of eV are also observed ([Peterson et al., 2008](#)). The complicated and often
550 multi-step processes involved in generating ion outflows are, in part, the consequence of the
551 external coupling of the magnetosphere with the solar wind. Moreover, studies of ion outflow
552 and ion composition in the magnetosphere are crucial because cold ions can be transported and
553 heated, influencing the ring current. The presence of cold ions can also influence reconnection
554 rates on the dayside and affect the properties and occurrence of plasma waves such as
555 Electromagnetic Ion Cyclotron (EMIC) waves. As shown by [Zong et al. \(2012\)](#), increases in ion
556 energy spectra from ~10 eV to ~40 eV are strongly correlated with the electric and magnetic
557 field components of ULF waves. Thus, with an enhanced number of shocks in SC25 and Arase
558 data covering at least the extension of SC25, a statistical study to investigate how changes in
559 energetic ion composition and their subsequent effects on the ring current and dayside
560 reconnection may be possibly accomplished.

561

562 **5.3 Ionosphere**

563

564 The increase or decrease in number of shocks impacting the Earth's magnetosphere nearly
565 directly translates into the number of geomagnetic storms which influences ionospheric
566 variability differently in high, mid, and equatorial latitude regions. In case of increased shock
567 numbers, the consequences on ionospheric variability are diverse ranging from increased
568 occurrence of ionospheric storm effects (e.g., [Matamba et al., 2015](#)) to more complexity in
569 ionospheric parameters' modelling such as TEC on both regional and global scales (e.g.,
570 [Uwamahoro & Habarulema 2015](#)). Anticipating the nature of this complexity is difficult as
571 different storms are driven by different physical processes. It is, however, known that increases
572 in electron density or TEC from its background values due to IP shock impacts (usually known
573 as the positive storm effect) are more difficult to model than negative storm effects which are
574 known to be linked to changes in thermospheric composition (e. g., [Fuller-Rowell et al., 1996](#)).
575 Additionally, depending on local daytime, prompt penetrating electric field of magnetospheric
576 origin can significantly alter equatorial electrodynamics. During local daytime, this leads to
577 enhanced eastward electric fields in the equatorial regions which increases the vertical $\mathbf{E} \times \mathbf{B}$
578 drift resulting in expansion of equatorial ionization anomaly towards mid latitudes through
579 equatorial ionospheric fountain effects (e.g., [Tsurutani et al., 2004](#)). Partly coupled to this, a
580 major determinant of the occurrence of post-sunset ionospheric irregularities is the equatorial
581 zonal electric field. Changes in the polarity and magnitude of this electric field have implications
582 on either enhanced occurrence or suppression of these ionospheric irregularities.

583

584 A stronger solar cycle with higher number of strong shocks could contribute to the understanding
585 of drivers triggering magnetospheric super substorms, events characterized with SuperMAG
586 westward auroral electrojet indices $SML < -2,500$ nT ([Hajra et al., 2016](#); [Tsurutani & Hajra,](#)
587 [2015](#); [Hajra & Tsurutani, 2018](#)). Although super substorm occurrences depend on pre-condition
588 states of the magnetosphere such as intense negative IMF B_z being sustained for some time
589 ([Craven et al., 1986](#); [Zhou & Tsurutani, 2001](#); [Yue et al., 2010](#)), super substorms do not
590 necessarily take place during magnetic storms of any intensity ([Tsurutani et al., 2015](#); [Tsurutani](#)

591 & Hajra, 2015; Hajra et al., 2016; Zong et al., 2021). Additionally, very intense GIC peaks at
592 high latitudes occur during super substorms (Oliveira et al., 2021; Tsurutani & Hajra, 2021;
593 2023; Oliveira et al., 2024a,b). Understanding triggering mechanisms of super substorms is
594 important because intense nighttime energetic particle injections, associated with large-scale,
595 localized ground dB/dt variations usually occur during such events (Ngwira et al., 2018; Oliveira
596 et al., 2021; 2024a,b). Therefore, a higher number of shocks observed during SC25 (including
597 more fast, nearly frontal shocks) will most likely contribute to the understanding of super
598 substorm triggering by shocks.

599
600 Multi-spacecraft measurements such as from the upcoming NASA Geospace Dynamics
601 Constellation (GDC) mission (Rowland et al., 2023) can complement ground-based
602 magnetometer measurements and further expand our understanding of the spatial and temporal
603 variations of the MI current systems and waves driven by IP shocks. For example, AMPERE
604 (Active Magnetosphere and Planetary Electrodynamics Response Experiment) is currently used
605 to provide global images of radial (approximate field-aligned) currents by fitting Iridium multi-
606 satellite magnetometer measurements to a set of base functions (Anderson et al., 2000). This
607 technique is appropriate to sample the larger scale and longer lasting currents excited by IP
608 shocks (e.g., Shi et al., 2019; Vines et al., 2023; Oliveira et al., 2024a,b), but not for the more
609 rapid and finer spatial scale currents and waves mentioned above. However, by incorporating
610 additional satellite magnetometer measurements such as from GDC, thus expanding in situ
611 magnetometer coverage, these global currents could potentially be provided more frequently and
612 for smaller spatial scales (Vines et al., 2023), thus lending themselves to exploring the more
613 rapid and finer scale variations related to shocks. As another example, when multi-satellite
614 constellations such as GDC are in a string-of-pearls configuration, their repeated and rapid
615 sampling of the same spatial region can be used to examine more rapid and localized
616 disturbances and waves excited by IP shocks, particularly when combined with contextual
617 ground-based observations such as magnetometers or radars (e.g., Pitout et al., 2015). Although
618 GDC was originally planned to launch in 2029, it may be launched later due to current funding
619 restrictions.

620
621 The Electrojet Zeeman Imaging Explorer (EZIE) mission (Yee et al., 2021; Laundal et al., 2022)
622 is a NASA mission that aims to study the ionospheric auroral and equatorial electrojets. The
623 three-satellite mission, planned to be launched October 2024, will use advanced imaging
624 techniques to study the structure and dynamics of the geomagnetic field within the ionosphere.
625 As described by Yee et al. (2017), EZIE will use the Zeeman splitting (Zeeman, 1897) of the O₂
626 thermal emission line at frequency of 118 GHz around 80 km altitude. Then, a vector magnetic
627 residual $\delta\mathbf{B}$ will be obtained by subtracting the ambient magnetic field computed with a
628 geomagnetic field model, from which an equivalent ionospheric current solution is derived to
629 investigate the structure and evolution of currents with scale sizes of ~100-1000 km, including
630 longitudinal variations (Yee et al., 2021; Laundal et al., 2022). By observing these currents,
631 EZIE will improve our understanding of the mechanisms behind space weather phenomena and
632 how they, e.g., affect satellite communications and navigation systems. Since EZIE is expected
633 to be in orbit for 18 months and considering the spacecraft will be launched in late 2024, and
634 accounting for the commissioning, from Figure 1, we estimate EZIE will observe 45-65 shocks
635 with an average of 55 events for SC25 (early 2025 to mid 2026). These numbers are higher than
636 the number of events observed in SC24 (41) in a similar period (early 2014 to mid 2015).

637 Therefore, we predict EZIE will have an opportunity to study a reasonable number of shock-
638 induced substorms, hopefully including some super substorm events described above because
639 SC25 will be stronger than SC24.

640

641 **5.4 Ground magnetometer response and GICs**

642

643 SC25 presents several opportunities for advancing our understanding of the complex spatial and
644 temporal variations in the ground magnetic response to IP shocks, including the excitation of
645 ULF waves. For example, [Araki et al., \(1997\)](#) noted when studying the SI⁺/sudden
646 commencement event from the 24 March 1991 IP shock/storm that 1 minute data was not
647 adequate to characterize the event. Many other studies have reinforced this point, finding that 1-
648 min samples are not sufficient for studying the rapid temporal variations, including pulsations,
649 that often occur in response to IP shocks (e.g., [Oliveira et al., 2020](#); [Hayakawa et al., 2022](#);
650 [Hartinger et al. 2023](#)). SC25 represents an opportunity to make progress in this area because
651 more ground magnetometers are now collecting and publishing data with 1-s sampling intervals
652 in comparison to past solar cycles (e.g., [Love & Finn, 2011](#); [Gjerloev, 2012](#)), enabling more
653 routine measurements of the rapid temporal variations excited by shocks. However, more
654 magnetometers with denser spatial coverage are still needed to examine mesoscale currents and
655 waves related to shocks that are localized in latitude or longitude (e.g., [Araki et al., 1997](#)). A
656 notable gap includes mid- and low-latitude regions in North America, where magnetometer
657 spatial coverage is relatively sparse yet large geomagnetic disturbances and GICs related to
658 shocks can occur (e.g., [Kappenman, 2003](#); [Caraballo et al., 2019](#)).

659

660 A higher number of IP shocks observed in SC25 could provide an opportunity to accomplish a
661 robust statistical study using European quasi-Meridional Magnetometer array (EMMA) data
662 ([Lichtenberger et al., 2013](#); [Del Corpo et al., 2019](#)). EMMA, consisting of 27 stations, is made
663 up by the extension of SEGMA (South European Geo Magnetic Array), MM100 (Magnetic
664 Meridian 100) and the Finnish part of IMAGE (International Monitor of Auroral
665 Geomagnetic Effects). These ground magnetic field data are then coupled with the MA.I.GIC
666 model ([Piersanti et al., 2019](#)) for the evaluation of geoelectric field response to shock impacts.
667 These predicted shocks for SC25 can provide a great opportunity for the use of EMMA data in a
668 robust and solid statistical analysis of geoelectric field response to shocks as a function of
669 magnetospheric L shells. For example, case studies and statistical analyses of ULF waves can
670 experimentally test a hypothesis suggested by [Oliveira et al. \(2020\)](#), in which the shock impact
671 angle affects the wave mode of the perturbation (nearly frontal shocks can trigger odd-mode
672 waves only, whereas highly inclined shocks can trigger both even- and odd-wave modes).
673 Additionally, these SC25 shock numbers can contribute to the prediction of GICs from mid- to
674 high-latitude Europe, since GICs at such latitudes can pose significant threats to power grids
675 ([Viljanen et al., 2014](#); [Torta et al., 2017](#); [Tozzi et al., 2019](#)).

676

677 New Zealand has been a particular focus in recent years, due to the relative abundance of
678 contemporaneous magnetic field and GIC measurements (e.g., [Mac Manus et al., 2017](#)) allowing
679 the building of validated modeling tools ([Mac Manus et al., 2022](#)). Further, in new Zealand's
680 recent history it has experienced severe space weather effects resulting from SI⁺ events; an

681 electrical transformer failed during the initial phase of a geomagnetic storm in November 2001
682 caused by a fast (presumably nearly frontal) IP shock (Marshall et al., 2012; Rodger et al., 2017;
683 Oliveira et al., 2018). The links uncovered between SI⁺ events and GICs are complex, with
684 several confounding parameters including the frequency content and orientation of the magnetic
685 field change (e.g., A.W. Smith et al., 2022; 2024). An increasing number of shocks in SC25
686 promises to help to untangle these drivers. Further, we expect that a greater number of
687 "significantly" geoeffective shocks will allow the testing of hypotheses, helping to understand
688 the types of shock-triggered SI⁺ events that are of most importance in terms of the ground impact
689 of space weather (e.g., Oliveira et al., 2018; 2024a,b; A.W. Smith et al., 2020).

690
691 The Embrace Magnetometer Network (Embrace MagNet) was developed to provide
692 measurements at low latitudes in a region bounded by 50° of latitude to 40° of longitude,
693 encompassing the eastern South American sector, aiming to provide subsidies to understand
694 geomagnetically active time evolution at low latitudes by comparing ground observations from
695 east to west, including storm time ionospheric disturbances (Denardini et al., 2018a; 2018b). As
696 an example, Silva et al. (2023) used Embrace MagNet to evaluate dB/dt amplitudes during
697 geomagnetic storms. They concluded that the magnetic field variations might have additional
698 contributions from the SAA over Embrace MagNet instruments. In this way, the perspective for
699 SC25 having a higher number of shocks in comparison to SC24 will provide the Embrace
700 MagNet instruments with a large number of events to better describe the MI conditions driving
701 pulsations and geoelectric field induction at low latitudes including the SAA region.

702
703 Enhancements of the equatorial electrojet current are important because they can also generate
704 ground dB/dt variations linked to GICs at low latitudes triggered by shocks (Carter et al., 2015;
705 Oliveira et al., 2018; Nilam & Tulasi Ram, 2022). Although not as intense as auroral and sub-
706 auroral dB/dt variations, these equatorial dB/dt variations can cause significant overtime effects
707 on power transmission lines of nations located in Southeast Asia, western Africa, and South
708 America near the magnetic equator (Moldwin et al., 2016). For example, Nilam et al. (2023)
709 used two ground magnetometer stations in southern India named Tirunelveli (TIR, 8.6°N, below
710 the equatorial electrojet), and Alibag (ABG, 18.6°N, outside the equatorial electrojet), to provide
711 an empirical relationship between shock parameters and the stations' local time. As an example
712 of further space weather-related applications, the empirical relationship provided by Nilam et al.
713 (2023) can be improved by introducing shock impact angle effects since they have significant
714 control of the geomagnetic activity triggered by shocks (Oliveira & Samsonov, 2018; Oliveira,
715 2023b). This analysis can be further improved by the inclusion of more shock events observed in
716 SC25 in comparison to the analysis previously performed by Nilam et al. (2023).

717
718 Variabilities of the magnetospheric and ionospheric currents described in Section 4 usually
719 generate induced currents in the solid Earth. As a result, geomagnetic field variations measured
720 by ground stations capture superposed field variations generated from the ionosphere and
721 magnetosphere and from the Earth's crust. Ionospheric equivalent currents are frequently located
722 ~100 km above the Earth's surface, and telluric currents are located 1 m below the Earth's
723 surface (Juusola et al., 2020; 2023). By using ground magnetometer data from the IMAGE array,
724 Juusola et al. (2020) showed that typically internal (telluric origin) dB/dt variations dominate
725 external (ionospheric origin) dB/dt variations because the former are much closer to the ground.

726 Because telluric currents are highly dependent on the local ground conductivity, interpretation of
727 the ionospheric equivalent currents and their magnetic field in terms of solar wind drivers
728 (including shocks) is more straightforward than interpretation of the unseparated magnetic field.
729 Thus, more shocks in SC25 will bring an opportunity to investigate and quantify telluric and
730 ionospheric current effects on ground dB/dt variations and their links to subsequently generated
731 GICs (Pulkkinen et al., 2017; Dimmock et al., 2020; Oliveira et al., 2024a,b).

732
733 As discussed above, while the predictions of shock occurrences in SC25 is useful from a
734 statistical point of view and instructive for future missions planning, this study does not advance
735 the possibility to predict space weather phenomena. This is out of this work's scope. However,
736 an increased number of shocks observed at L1 during SC25 will provide a great opportunity for
737 the improvement of shock detection tools for further space weather alerts (Kruparova et al.,
738 2013; Cash et al., 2014; Carter et al., 2022). Such alerts can be used, e.g., by power plant
739 operators to take actions to avoid long-term detrimental effects caused GICs on ground
740 equipment, particularly for shocks that are forecasted to impact Earth nearly frontally (Oliveira et
741 al., 2018; 2021).

742
743 Finally, our shock count predictions and space weather research opportunities discussed in this
744 article indicate that SC25 will be different from SC24 when comparing availability of shock
745 events and several data sets provided by spacecraft missions in the solar wind, magnetosphere,
746 ionosphere, and ground magnetometers. However, since space weather is highly cross-
747 disciplinary, as also suggested by Ledvina et al. (2022), SC25 will bring great opportunities for
748 space weather research, but risk and resiliency approaches should be considered. Ledvina et al.
749 (2022) highlight three approaches to successfully address complex and inter-disciplinary
750 problems in space weather to mitigate eventual risks: 1) share open-data and data science
751 through open access and collaboration (McGranaghan et al., 2017); 2) develop cross-disciplinary
752 science and information systems by using multi-instrument investigations (as discussed in this
753 article) and deep-learning or artificial intelligence analyses (Camporeale, 2019); and 3) engage in
754 citizen science, an approach that connects scientists and the general public as a collaboration to
755 achieve scientific goals that go beyond the academia (Shirky, 2010).

756 757 **6. Conclusion**

758
759 In this work, we discussed two aspects of IP shock research and space weather applications.
760 Firstly, we used sunspot number data and shock data along with three models for sunspot number
761 predictions for SC25 to predict shock occurrence numbers for SC25. Secondly, we briefly
762 discussed many research opportunities that already are and will be available for shock research
763 and forecasting. We found that the number of shocks will be ~50% higher in SC25 in
764 comparison to SC24, with predictions ranging from ~40%-55% higher. With the unprecedented
765 number of simultaneously operating satellite missions in the solar wind, magnetosphere, and the
766 ionosphere, along with a large number of ground magnetic field and GIC data sets, we predict
767 SC25 will bring great opportunities for studies involving space weather research and forecasting.
768 In addition, we predict that a stronger solar cycle will produce more nearly frontal shocks that
769 are important for space weather research because they usually are more geoeffective than highly

770 inclined shocks due to quasi-symmetric magnetospheric compressions (Oliveira & Samsonov,
771 2018; Oliveira, 2023b). Finally, we also encouraged IP shock studies involving multi-instrument
772 analyses. However, since space weather is highly cross-disciplinary, we suggested the
773 assessment of risk and resiliency should be considered in such studies (Ledvina et al., 2022).

774

775 **Acknowledgments**

776 DMO thanks financial support provided by NASA through the Heliophysics Guest Investigation-
777 Open (HGIO) program (grant number 80NSSC22K0756), and through the Living with a Star
778 (LWS) program (grant number NNH22ZDA001N-LWS). CPF acknowledges NASA grant
779 80NSSC21K0584. MDH acknowledges support from NSF AGS-2027210 and NASA
780 80NSSC19K0907. JMW and EZ acknowledge financial support from NASA 80NSSC22K0756.

781

782 **Data availability statement**

783 The IP shock list is available at the Zenodo repository described in Oliveira (2023c). The
784 SILSO/SSN data can be collected from the website <https://www.sidc.be/SILSO/datafiles>. The
785 MC sunspot number data can be downloaded from the HELIO4CAST website
786 <https://helioforecast.space/solarcycle>. The UH sunspot data are available at the Solar Cycle
787 Science website (<http://solarcyclescience.com/forecasts.html>). The NOAA sunspot data are
788 available at <https://www.swpc.noaa.gov/products/solar-cycle-progression>. The F10.7 solar index
789 data used in the Supporting Information (daily and yearly data from January 1964 to December
790 2023) were downloaded from the NASA OMNI website
791 (<https://omniweb.gsfc.nasa.gov/form/dx1.html>).

792

793

794 **References**

795 Akasofu, S.-I., & Chao, J. (1980). Interplanetary shock waves and magnetospheric substorms.
796 *Planetary and Space Science*, 28 (4), 381-385. [https://doi.org/10.1016/0032-](https://doi.org/10.1016/0032-0633(80)90042-2)
797 [0633\(80\)90042-2](https://doi.org/10.1016/0032-0633(80)90042-2)

798 Alken, P., Thébault, E., Beggan, C. D., Amit, H., Aubert, J., Baerenzung, J., Bondar, T. N.,
799 Brown, W. J., Califf, S., Chambodut, A., Chulliat, A., Cox, G. A., Finlay, C. C., Fournier,
800 A., Gillet, N., Grayver, A., Hammer, M. D., Holschneider, M., Huder, L., Hulot, G.,
801 Jager, T., Kloss, C., Korte, M., Kuang, W., Kuvshinov, A., Langlais, B., Léger, J.-M.,
802 Lesur, V., Livermore, P. W., Lowes, F. J., Macmillan, S., Magnes, W., Manda, M.,
803 Marsal, S., Matzka, J., Metman, M. C., Minami, T., Morschhauser, A., Mound, J. E.,
804 Nair, M., Nakano, S., Olsen, N., Pavón-Carrasco, F. J., Petrov, V. G., Ropp, G., Rother,
805 M., Sabaka, T. J., Sanchez, S., Saturnino, D., Schnepf, N. R., Shen, X., Stolle, C.,
806 Tangborn, A., Tøffner-Clausen, L., Toh, H., Torta, J. M., Varner, J., Vervelidou, F.,
807 Vigneron, P., Wardinski, I., Wicht, J., Woods, A., Yang, Y., Zeren, Z., & Zhou, B.

- 808 (2021). International geomagnetic reference field: the thirteenth generation. *Earth,*
809 *Planets and Space*, 73 (49). <https://doi.org/10.1186/s40623-020-01288-x>
- 810 Anderson, B. J., Takahashi, K., & Toth, B. A. (2000). Sensing global Birkeland currents with
811 Iridium® engineering magnetometer data. *Geophysical Research Letters*, 27(24), 4045-
812 4048. <https://doi.org/10.1029/2000GL000094>
- 813 Andrioli, V. F., Echer, E., Savian, J. F., & Schuch, N. J. (2006). Positive and negative sudden
814 impulses caused by fast forward and reverse interplanetary shocks. *Revista Brasileira de*
815 *Geofísica*, 25(2), 175-179. <https://doi.org/10.1590/S0102-261X2007000600021>
- 816 Andriyas, T. (2017). A comparative study of sawtooth events and substorm onsets triggered by
817 interplanetary shocks. *Annals of Geophysics*, 60(6), GM672, 1-12.
818 <https://doi.org/10.4401/ag-7481>
- 819 Araki, T. (1977). Global structure of geomagnetic sudden commencements. *Planetary and Space*
820 *Science*, 25(4), 373-384. [https://doi.org/10.1016/0032-0633\(77\)90053-8](https://doi.org/10.1016/0032-0633(77)90053-8)
- 821 Araki, T., Fujitani, S., Emoto, M., Yumoto, K., Shiokawa, K., Ichinose, T., Luehr, H., Orr, D.,
822 Milling, D. K., Singer, H., Rostoker, G., Tsunomura, S., Yamada, Y., & Liu, C. F.
823 (1997). Anomalous sudden commencement on March 24, 1991. *Journal of Geophysical*
824 *Research*, 102(A7), 14075-14086. <https://doi.org/10.1029/96JA03637>
- 825 Arcimis, A. (1903). Telegraphic Disturbances in Spain on October 31. *Nature*, 69(1776), 29.
826 <https://doi.org/10.1038/069029b0>
- 827 Baker, D. N., Erickson, P. J., Fennell, J. F., Foster, J. C., Jaynes, A. N., & Verronen, P. T.
828 (2018). Space Weather Effects in the Earth's Radiation Belts. *Space Science Reviews*,
829 214 (17). <https://doi.org/10.1007/s11214-017-0452-7>
- 830 Balogh, A., Bothmer, V., Crooker, N. U., Forsyth, R. J., Gloeckler, G., Hewish, A., Hilchen-
831 bach, M., Kallenbach, R., Klecker, B., Linker, J., Lucek, E., Mann, G., Marsch, E.,
832 Posner, A., Richardson, I., Schmidt, J., Wang, M. S. Y.-M., Aellig, R. W.-S. M. R.,
833 Bochsler, P., Hefti, S., & Mikić, Z. (1999). The solar origin of corotating interaction
834 regions and their formation in the inner heliosphere. *Space Science Reviews*, 89(1), 141-
835 178. <https://doi.org/10.1023/A:1005245306874>
- 836 Bame, S. J., Asbridge, J. R., Feldman, W. C., Fenimore, E. E., & Gosling, J. T. (1979). Solar
837 wind heavy ions from flare-heated coronal plasma. *Solar Physics*, 62 (1).
838 <https://doi.org/10.1007/BF00150143>
- 839 Barbosa, C., Alves, L., Caraballo, R., Hartmann, G. A., Papa, A. R. R., & Pirjola, R. J. (2015).
840 Analysis of geomagnetically induced currents at a low-latitude region over the solar
841 cycles 23 and 24: comparison between measurements and calculations. *Journal of Space*
842 *Weather and Space Climate*, 5(A35). <https://doi.org/10.1051/swsc/2015036>

- 843 Barlow, W. H. (1849). VI. On the spontaneous electrical currents observed in the wires of the
844 electric telegraph. *Philosophical Transactions of the Royal Society of London*, 61–72.
845 <https://doi.org/10.1098/rstl.1849.0006>
- 846 Benvenuto, F., Piana, M., Campi, C., & Massone, A. M. (2018). A Hybrid
847 Supervised/Unsupervised Machine Learning Approach to Solar Flare Prediction. *The*
848 *Astrophysical Journal*, 853(1). <https://doi.org/10.3847/1538-4357/aaa23c>
- 849 Bhowmik, P., & Nandy, D. (2018). Prediction of the strength and timing of sunspot cycle 25
850 reveal decadal-scale space environmental conditions. *Nature Communications*, 9 (5209).
851 <https://doi.org/10.1038/s41467-018-07690-0>
- 852 Bhowmik, P., Jiang, J., Upton, L., Lemerle, A., & Nandy, D. (2023). Physical Models for Solar
853 Cycle Predictions. *Space Science Reviews*, 219(40). [https://doi.org/10.1007/s11214-023-](https://doi.org/10.1007/s11214-023-00983-x)
854 [00983-x](https://doi.org/10.1007/s11214-023-00983-x)
- 855 Bishop, C. M. (2016). *Pattern Recognition and Machine Learning*. New York, NY: Springer.
- 856 Blake, J. B., Kolasinski, W. A., Fillius, R. W., & Mullen, E. G. (1992). Injection of electrons and
857 protons with energies of tens of MeV into L < 3 on 24 March 1991. *Geophysical*
858 *Research Letters*, 19(8), 821-824. <https://doi.org/10.1029/92GL00624>
- 859 Borovsky, J. E., & Denton, M. H. (2006). Differences between CME-driven storms and CIR-
860 driven storms. *Journal of Geophysical Research*, 111 (A7).
861 <https://doi.org/10.1029/2005JA011447>
- 862 Boteler, D. H., & Pirjola, R. J. (2017). Modeling geomagnetically induced currents. *Space*
863 *Weather*, 15(1), 258-276. <https://doi.org/10.1002/2016SW001499>
- 864 Boteler, D. H., Chakraborty, S., Shi, X., Hartinger, M. D., & Wang, X. (2024). An Examination
865 of Geomagnetic Induction in Submarine Cables. *Space Weather*, 22 (2),
866 e2023SW003687. <https://doi.org/10.1029/2023SW003687>
- 867 Burton, R. K., McPherron, R. L., & Russell, C. T. (1975). An empirical relationship between
868 interplanetary conditions and Dst. *Journal of Geophysical Research*, 80(31), 4204–4214.
869 <https://doi.org/10.1029/JA080i031p04204>
- 870 Byrne, J. P., Maloney, S. A., McAteer, R. T. J., Refojo, J. M., & Gallagher, P. T. (2010).
871 Propagation of an earth-directed coronal mass ejection in three dimensions. *Nature*
872 *Communications*, 1(74). <https://doi.org/10.1038/ncomms1077>
- 873 Cahill, L. J., & Amazeen, P. (1963). The boundary of the geomagnetic field. *Journal of*
874 *Geophysical Research*, 68(7), 1835—1843. <https://doi.org/10.1029/JZ068i007p01835>

- 875 Campbell, W. H. (1980). Observation of electric currents in the Alaska oil pipeline resulting
876 from auroral electrojet current sources. *Geophysical Journal International*, 61(2), 437-
877 449. <https://doi.org/10.1111/j.1365-246X.1980.tb04325.x>
- 878 Camporeale, E. (2019). The challenge of machine learning in space weather: Nowcasting and
879 forecasting. *Space Weather*, 17 (8), 1166-1207. <https://doi.org/10.1029/2018SW002061>
- 880 Caraballo, R., González-Esparza, J. A., Sergeeva, M., & Pacheco, C. R. (2020). First GIC
881 Estimates for the Mexican Power Grid. *Space Weather*, 18 (2), e2019SW002260.
882 <https://doi.org/10.1029/2019SW002260>
- 883 Carter, B. A., Yizengaw, E., Pradipta, R., Halford, A. J., Norman, R., & Zhang, K. (2015).
884 Interplanetary shocks and the resulting geomagnetically induced currents at the equator.
885 *Geophysical Research Letters*, 42 (16), 6554–6559.
886 <https://doi.org/10.1002/2015GL065060>
- 887 Carter, B. A., Iles, G. N., Raju, R., Afful, A. M., Maj, R., Dao, T., Terkildsen, M., Lobzin, V.,
888 Bouya, Z., Parkinson, M., Le May, S., Choy, S., Hordyniec, P., Hordyniec, B., Currie, J.,
889 Skov, T., & Peake, I. D. (2022). RMIT University’s practical space weather prediction
890 laboratory. *Journal of Space Weather and Space Climate*, 12(28), 20.
891 <https://doi.org/10.1051/swsc/2022025>
- 892 Cash, M. D., Wrobel, J. S., Cosentino, K. C., & Reinard, A. A. (2014). Characterizing
893 interplanetary shocks for development and optimization of an automated solar wind
894 shock detection algorithm. *Journal of Geophysical Research*, 119(6), 4210-4222.
895 <https://doi.org/10.1002/2014JA019800>
- 896 Chakraborty, S., Boteler, D. H., Shi, X., Murphy, B. S., Hartinger, M. D., Wang, X., Lucas, G.,
897 & Bake, J. B. H. (2022). Modeling geomagnetic induction in submarine cables. *Frontiers*
898 *in Astronomy and Space Science*, 10 (1022475).
899 <https://doi.org/10.3389/fphy.2022.1022475>
- 900 Chapman, S., & Ferraro, V. C. A. (1931). A new theory of magnetic storms. *Terrestrial*
901 *Magnetism and Atmospheric Electricity*, 36 (2), 77-97.
902 <https://doi.org/10.1029/TE036i002p00077>
- 903 Chapman, S. C., Horne, R. B., & Watkins, N. W. (2020). Using the aa index over the last 14
904 solar cycles to characterize extreme geomagnetic activity. *Geophysical Research Letters*,
905 47(3), e2019GL086524. <https://doi.org/10.1029/2019GL086524>
- 906 Chen, X., Zong, Q., Hao, Y., Li, Q., Zhang, D., & Zhang, H. (2023). Propagation of the Inter-
907 planetary Shock Induced Pulse: New Observations by the Global Navigation Satellite
908 System. *Journal of Geophysical Research: Space Physics*, 128(1), e2022JA030975.
909 <https://doi.org/10.1029/2022JA030975>

- 910 Clette, F., Lefvère, L., Chatzistergos, T., Hayakawa, H., Carrasco, V. M. S., Arlt, R., Cliver, E.
911 W., Dudok de Wit, T., Friedli, T. K., Karachik, N., Kopp, G., Lockwood, M., Mathieu,
912 S., Muñoz-Jaramillo, A., Owens, M., Pesnell, D., Pevtsov, A., Svalgaard, L., Usoskin, I.
913 G., van Driel-Gesztelyi, L., & Vaquero, J. M. (2023). Recalibration of the Sunspot-
914 Number: Status Report. *Solar Physics*, 298(44). [https://doi.org/10.1007/s11207-023-](https://doi.org/10.1007/s11207-023-02136-3)
915 02136-3
- 916 Collier, M. R., Lepping, R. P., & Berdichevsky, D. B. (2007). A statistical study of
917 interplanetary shocks and pressure pulses internal to magnetic clouds. *Journal of*
918 *Geophysical Research*, 112(A6). <https://doi.org/10.1029/2006JA011714>
- 919 Cowley, S. W. H. (2000). Magnetosphere-ionosphere interactions: A tutorial review. In S.
920 Ohtani, R. Fujii, M. Hesse, & R. L. Lysak (Eds.), *Magnetospheric Current Systems*,
921 Geophysical Monograph Series (Vol. 118, p. 91-106). Washington, D.C.: American
922 Geophysical Union. <https://doi.org/10.1029/GM118p0091>
- 923 Craven, J. D., Frank, L. A., Russell, C. T., Smith, E. E., & Lepping, R. P. (1986). Global auroral
924 responses to magnetospheric compressions by shocks in the solar wind: Two case studies.
925 In Y. Kamide & J. A. Slavin (Eds.), *Solar Wind-Magnetosphere Coupling* (p. 367-380).
926 Tokyo, Japan: Terra Scientific.
- 927 Del Corpo, A., Vellante, M., Heilig, B., Pietropaolo, E., Reda, J., & Lichtenberger, J. (2019).
928 Observing the Cold Plasma in the Earth's Magnetosphere with the EMMA Network.
929 *Annals of Geophysics*, 62(4), 1-19. <https://doi.org/10.4401/ag-7751>
- 930 Denardini, C. M., Chen, S. S., Resende, L. C. A., Moro, J., Bilibio, A. V., Fagundes, P. R.,
931 Gende, M. A., Cabrera, M. A., Bolzan, M. J. A., Padilha, A. L., Schuch, N. J.,
932 Hormaechea, J. L., Alves, L. R., Barbosa Neto, P. F., Nogueira, P. A. B., Picanço, G. A.
933 S., & Bertolotto, T. O. (2018a). The Embrace Magnetometer Network for South
934 America: Network Description and Its Qualification. *Radio Science*, 53(3), 288-302.
935 <https://doi.org/https://doi.org/10.1002/2017RS006477>
- 936 Denardini, C. M., Chen, S. S., Resende, L. C. A., Moro, J., Bilibio, A. V., Fagundes, P. R.,
937 Gende, M. A., Cabrera, M. A., Bolzan, M. J. A., Padilha, A. L., Schuch, N. J.,
938 Hormaechea, J. L., Alves, L. R., Barbosa Neto, P. F., Nogueira, P. A. B., Picanço, G. A.
939 S., & Bertolotto, T. O. (2018b). The Embrace Magnetometer Network for South
940 America: Network Description and Its Qualification. *Radio Science*, 53 (3), 288-302.
941 <https://doi.org/10.1002/2017RS006477>
- 942 Dimmock, A. P., Rosenqvist, L., Welling, D. T., Viljanen, A., Honkonen, I., Boynton, R. J., &
943 Yordanova, E. (2020). On the Regional Variability of dB/dt and Its Significance to GIC.
944 *Space Weather*, 18 (8), e2020SW002497. <https://doi.org/10.1029/2020SW002497>
- 945 Dong, X.-C., Dunlop, M. W., Wang, T.-Y., Cao, J.-B., Trattner, K. J., Bamford, R., Russell, C.
946 T., Bingham, R., Strangeway, R. J., Fear, R. C., Giles, B. L., & Torbert, R. B. (2018).

- 947 Carriers and sources of magnetopause current: MMS case study. *Journal of Geophysical*
948 *Research: Space Physics*, 123 (7), 5464-5475. <https://doi.org/10.1029/2018JA025292>
- 949 Echer, E., Gonzalez, W. D., Vieira, L. E. A., Dal Lago, A., Guarnieri, F. L., Prestes, A.,
950 Gonzalez, A. L. C., & Schuch, N. J. (2003). Interplanetary shock parameters during solar
951 activity maximum (2000) and minimum (1995-1996). *Brazilian Journal of Physics*,
952 33(1), 115-122. <https://doi.org/10.1590/S0103-97332003000100010>
- 953 Finlay, C. C., Kloss, C., Olsen, N., Magnus D. Hammer, L. T.-C., Grayver, A., & Kuvshinov, A.
954 (2020). The CHAOS-7 geomagnetic field model and observed changes in the South
955 Atlantic Anomaly. *Earth, Planets and Space*, 72(1), 1-31.
956 <https://doi.org/10.1186/s40623-020-01252-9>
- 957 Fiori, R. A. D., Boteler, D. H., & Gillies, D. M. (2014). Assessment of GIC risk due to
958 geomagnetic sudden commencements and identification of the current systems
959 responsible. *Space Weather*, 12 (1), 76-91. <https://doi.org/10.1002/2013SW000967>
- 960 Fogg, A. R., Jackman, C. M., Coco, I., Douglas Rooney, L., Weigt, D. M., & Lester, M. (2023).
961 Why are some solar wind pressure pulses followed by geomagnetic storms? *Journal of*
962 *Geophysical Research: Space Physics*, 128(8), e2022JA031259.
963 <https://doi.org/10.1029/2022JA031259>
- 964 Fogtman, A., Baatout, S., Baselet, B., Berger, T., Hellweg, C. E., Jiggins, P., Tessa, C. L.,
965 Narici, L., Nieminen, P., Sabatier, L., Santin, G., Schneider, U., Straube, U., Tabury, K.,
966 Tinganelli, W., Walsh, L., & Durante, M. (2023). Towards sustainable human space
967 exploration-priorities for radiation research to quantify and mitigate radiation risks. *npj*
968 *Microgravity*, 9 (8). <https://doi.org/10.1038/s41526-023-00262-7>
- 969 Forbes, J. M. (1981). The equatorial electrojet. *Reviews of Geophysics*, 19(3), 469–504.
970 <https://doi.org/10.1029/RG019i003p00469>
- 971 Fukushima, N. (1994). Some topics and historical episodes in geomagnetism and aeronomy.
972 *Journal of Geophysical Research*, 99(A10). <https://doi.org/10.1029/94JA0010>
- 973 Fuller, S., Lehnhardt, E., Zaid, C., & Halloran, K. (2022). Gateway program status overview.
974 *Journal of Space Safety Engineering*, 9 (4), 625-628.
975 <https://doi.org/10.1016/j.jsse.2022.07.008>
- 976 Fuller-Rowell, T. J., Codrescu, M. V., Rishbeth, H., Moffett, R. J., & Quegan, S. (1996). On the
977 seasonal response of the thermosphere and ionosphere to geomagnetic storms. *Journal of*
978 *Geophysical Research*, 101 (A2), 2343–2353. <https://doi.org/10.1029/95JA01614>
- 979 Fuselier, S. A., Ghielmetti, A. G., Moore, T. E., Collier, M. R., Quinn, J. M., Wil- son, G. R.,
980 Wurz, P., Mende, S. B., Frey, H. U., Jamar, C., Gerard, J.-C., & Burch, J. L. (2001). Ion
981 outflow observed by IMAGE: Implications for source regions and heating mechanisms.

- 982 *Geophysical Research Letters*, 28 (6), 1163-1166.
983 <https://doi.org/10.1029/2000GL012450>
- 984 Gaunt, C., & Coetzee, G. (2007). Transformer failures in regions incorrectly considered to have
985 low GIC-risk. In *Power Tech, 2007 IEEE Lausanne* (pp. 807–812). Lausanne,
986 Switzerland: IEEE. <https://doi.org/10.1109/PCT.2007.4538419>
- 987 Gjerloev, J. W. (2012). The SuperMAG data processing technique. *Journal of Geophysical*
988 *Research*, 117(A09213), 1–19. <https://doi.org/10.1029/2012JA017683>
- 989 Gkioulidou, M., Ohtani, S., Ukhorskiy, A. Y., Mitchell, D. G., Takahashi, K., Spence, H. E.,
990 Wygant, J. R., Kletzing, C. A., & Barnes, R. J. (2019). Low-Energy (V keV) O⁺ Ion
991 Outflow Directly Into the Inner Magnetosphere: Van Allen Probes Observations. *Journal*
992 *of Geophysical Research: Space Physics*, 124 (1), 405-419.
993 <https://doi.org/https://doi.org/10.1029/2018JA025862>
- 994 Gledhill, J. A. (1976). Aeronomic effects of the South Atlantic Anomaly. *Reviews of Geophysics*,
995 14(2), 173-187. <https://doi.org/10.1029/RG014i002p00173>
- 996 Gopalswamy, N., Michalek, G., Yashiro, S., Mäkelä, P., Akiyama, S., & Xie, H. (2023). What
997 Do Halo CMEs Tell Us about Solar Cycle 25? *The Astrophysical Journal Letters*,
998 952(L13). <https://doi.org/10.3847/2041-8213/acdde2>
- 999 Gosling, J. T. (1997). Coronal mass ejections: An overview. In N. Crooker, J. A. Jockelyn, & J.
1000 Feynman (Eds.), *Coronal Mass Ejections*, Geophysical Monograph Series (Vol. 99, p. 9-
1001 16). Washington, D.C.: American Geophysical Union.
1002 <https://doi.org/10.1029/GM099p0009>
- 1003 Goyal, S. K., Kumar, P., and S. V. Vadawale, P. J., Sarkar, A., Shanmugam, M., Subra-
1004 manian, K. P., Bapat, B., Chakrabarty, D., Adhyaru, P. R., Patel, A. R., Banerjee, S. B., Shah, M.
1005 S., Tiwari, N. K., Adalja, H. L., Ladiya, T., Dadhania, M. B., Sarda, A., Hait, A. K.,
1006 Chauhan, M., & Bhavsar, R. R. (2018). Aditya Solarwind Particle EXperiment (ASPEX)
1007 onboard the Aditya-L1 mission. *Planetary and Space Science*, 163, 42-55.
1008 <https://doi.org/10.1016/j.pss.2018.04.008>
- 1009 Green, J. L., Dong, C., Jesse, M., Young, C. A., & Airapetian, V. (2022). Space weather
1010 observations, modeling, and alerts in support of human exploration of Mars. *Frontiers in*
1011 *Astronomy and Space Science*, 9 (1023305). <https://doi.org/10.3389/fspas.2022.1023305>
- 1012 Gummow, R. A., & Eng, P. (2002). GIC effects on pipeline corrosion and corrosion control
1013 systems. *Journal of Atmospheric and Solar-Terrestrial Physics*, 64(16), 1755-1764.
1014 [https://doi.org/10.1016/S1364-6826\(02\)00125-6](https://doi.org/10.1016/S1364-6826(02)00125-6)
- 1015 Hajra, R., Tsurutani, B. T., Echer, E., Gonzalez, W. D., & Gjerloev, J. W. (2016).
1016 Supersubstorms (SML < -2500 nT): Magnetic storm and solar cycle dependences.

- 1017 *Journal of Geophysical Research: Space Physics*, 121 (8), 7805-7816.
 1018 <https://doi.org/10.1002/2015JA021835>
- 1019 Hajra, R., & Tsurutani, B. T. (2018a). Interplanetary Shocks Inducing Magnetospheric
 1020 Supersubstorms (SML < -2500 nT): Unusual Auroral Morphologies and Energy Flow.
 1021 *The Astrophysical Journal*, 858(123). <https://doi.org/10.3847/1538-4357/aabaed>
- 1022 Hale, G. E., & Nicholson, S. B. (1925). The Law of Sun-Spot Polarity. *The Astrophysical*
 1023 *Journal*, 62, 270. <https://doi.org/10.1086/142933>
- 1024 Halekas, J. S., Poppe, A. R., McFadden, J. P., Angelopoulos, V., Glassmeier, K.-H., & Brain, D.
 1025 A. (2014). Evidence for small-scale collisionless shocks at the Moon from ARTEMIS.
 1026 *Geophysical Research Letters*, 41(21), 7436-7443.
 1027 <https://doi.org/10.1002/2014GL061973>
- 1028 Harten, R., & Clark, K. (1995). The design features of the GGS wind and polar spacecraft. *Space*
 1029 *Science Reviews*, 71, 22-40. <https://doi.org/10.1007/BF00751324>
- 1030 Hartinger, M. D., Takahashi, K., Drozdov, A. Y., Shi, X., Usanova, M. E., & Kress, B. (2022).
 1031 ULF Wave Modeling, Effects, and Applications: Accomplishments, Recent Advances,
 1032 and Future. *Frontiers in Astronomy and Space Science*, 9 (867394).
 1033 <https://doi.org/10.3389/fspas.2022.867394>
- 1034 Hartinger, M. D., Shi, X., Rodger, C. J., Fujii, I., Rigler, E. J., Kappler, J., Karl and Matzka,
 1035 Love, J. J., Baker, J. B. H., Mac Manus, D. H., Dalzell, M., & Petersen, T. (2023).
 1036 Determining ULF Wave Contributions to Geomagnetically Induced Currents: The
 1037 Important Role of Sampling Rate. *Space Weather*, 21(5), e2022SW003340.
 1038 <https://doi.org/https://doi.org/10.1029/2022SW003340>
- 1039 Hartmann, G. A., & Pacca, I. G. (2009). Time evolution of the South Atlantic Magnetic
 1040 Anomaly. *Anais da Academia Brasileira de Ciências*, 81 (2), 243-255.
 1041 <https://doi.org/10.1590/S0001-37652009000200010>
- 1042 Hathaway, D. H. (2015). The Solar Cycle. *Living Reviews in Solar Physics*, 12(4).
 1043 <https://doi.org/10.1007/lrsp-2015-4>
- 1044 Hayakawa, H., Ribeiro, P., Vaquero, J. M., Gallego, M. C., Knipp, D. J., Mekhaldi, F., Bhaskar,
 1045 A., Oliveira, D. M., Notsu, Y., Carrasco, V. M. S., Caccavari, A., Veenadhari, B.,
 1046 Mukherjee, S., & Ebihara, Y. (2020a). The Extreme Space Weather Event in 1903
 1047 October/November: An Outburst from the Quiet Sun. *The Astrophysical Journal Letters*,
 1048 897(1), L10. <https://doi.org/10.3847/2041-8213/ab6a18>
- 1049 Hayakawa, H., Besser, B. P., Iju, T., Arlt, R., Uneme, S., Imada, S., Bourdin, P.-A., & Kraml, A.
 1050 (2020). Thaddäus Derfflinger's Sunspot Observations during 1802–1824: A Primary
 1051 Reference to Understand the Dalton Minimum. *The Astrophysical Journal*, 890(2), 98.
 1052 <https://doi.org/10.3847/1538-4357/ab65c9>

- 1053 Hayakawa, H., Oliveira, D. M., Shea, M. A., Smart, D. F., Blake, S. P., Hattori, K., Bhaskar, A.
 1054 T., Curto, J. J., Franco, D. R., & Ebihara, Y. (2022). The Extreme Solar and Geomagnetic
 1055 Storms on 1940 March 20-25. *Monthly Notices of the Royal Astronomical Society*,
 1056 517(2), 1709-1723. <https://doi.org/10.1093/mnras/stab3615>
- 1057 Hazra, G., Nandy, D., Kitchatinov, L., & Choudhuri, A. R. (2023). Mean Field Models of Flux
 1058 Transport Dynamo and Meridional Circulation in the Sun and Stars. *Space Science*
 1059 *Reviews*, 219(39). <https://doi.org/10.1007/s11214-023-00982-y>
- 1060 Heirtzler, J. R. (2002). The future of the South Atlantic anomaly and implications for radiation
 1061 damage in space. *Journal of Atmospheric and Solar-Terrestrial Physics*, 64(16), 1701-
 1062 1708. [https://doi.org/10.1016/S1364-6826\(02\)00120-7](https://doi.org/10.1016/S1364-6826(02)00120-7)
- 1063 Heirtzler, J. R., Allen, J. H., & Wilkinson, D. C. (2002). Ever-present South Atlantic Anomaly
 1064 damages spacecraft. *Eos Transactions AGU*, 83 (15), 165-169.
 1065 <https://doi.org/10.1029/2002EO000105>
- 1066 Iban, M. C., & Şentürk, E. (2022). Machine learning regression models for prediction of multiple
 1067 ionospheric parameters. *Advances in Space Research*, 69 (3), 1319-1334.
 1068 <https://doi.org/10.1016/j.asr.2021.11.026>
- 1069 Jian, L., Russell, C., Luhmann, J., & Skoug, R. (2006b). Properties of stream interactions at one
 1070 AU during 1995-2004. *Solar Physics*, 239 (1-2), 337-392.
 1071 <https://doi.org/10.1007/s11207-006-0132-3> jurac
- 1072 Jurac, S., Kasper, J. C., Richardson, J. D., & Lazarus, A. J. (2002). Geomagnetic disturbances
 1073 and their relationship to interplanetary shock parameters. *Geophysical Research Letters*,
 1074 29(10). <https://doi.org/10.1029/2001GL014034>
- 1075 Juusola, L., Heikki Vanhamäki, A. V., & Smirnov, M. (2020). Induced currents due to 3D
 1076 ground conductivity play a major role in the interpretation of geomagnetic variations.
 1077 *Annales Geophysicae*, 30(5), 983-998. <https://doi.org/10.5194/angeo-38-983-2020>
- 1078 Juusola, L., Viljanen, A., Dimmock, A. P., Kellinsalmi, M., Schillings, A., & Weygand, J. M.
 1079 (2023). Drivers of rapid geomagnetic variations at high latitudes. *Annales Geophysicae*,
 1080 41(1), 13-27. <https://doi.org/10.5194/angeo-41-13-2023>
- 1081 Kaiser, M. L. (2005). The STEREO mission: an overview. *Advances in Space Research*, 36(8),
 1082 1483-1488. <https://doi.org/10.1016/j.asr.2004.12.066>
- 1083 Kanekal, S. G., Baker, D. N., Fennell, J. F., Jones, A., Schiller, Q., Richardson, I. G., Li, X.,
 1084 Turner, D. L., Califf, S., Claudepierre, S. G., Wilson III, L. B., Jaynes, A., Blake, J. B.,
 1085 Reeves, G. D., Spence, H. E., Kletzing, C. A., & Wygant, J. R. (2016). Prompt
 1086 acceleration of magnetospheric electrons to ultrarelativistic energies by the 17 March
 1087 2015 interplanetary shock. *Journal of Geophysical Research: Space Physics*, 121(8),
 1088 7622-7635. <https://doi.org/10.1002/2016JA022596>

- 1089 Kanekal, S., & Miyoshi, Y. (2021). Dynamics of the terrestrial radiation belts: a re- view of
 1090 recent results during the VarSITI (Variability of the Sun and Its Terrestrial Impact) era,
 1091 2014–2018. *Progress in Earth and Planetary Science*, 8 (35).
 1092 <https://doi.org/10.1186/s40645-021-00413-y>
- 1093 Kappenman, J. G. (2003). Storm sudden commencement events and the associated geo-
 1094 magnetically induced current risks to ground-based systems at low-latitude and mid-
 1095 latitude locations. *Space Weather*, 1 (3). <https://doi.org/10.1029/2003SW000009>
- 1096 Kasran, F. A. M., Jusoh, M. H., Adhikari, B., & Rahim, S. A. E. A. (2019). Field- aligned
 1097 currents (FACs) behaviour during the arrival of interplanetary magnetic shock. *Journal of*
 1098 *Physics: Conference Series*, 1152 (012027). [https://doi.org/10.1088/1742-](https://doi.org/10.1088/1742-6596/1152/1/012027)
 1099 [6596/1152/1/012027](https://doi.org/10.1088/1742-6596/1152/1/012027)
- 1100 Kelbert, A., & Lucas, G. M. (2020). Modified GIC Estimation Using 3-D Earth Conductivity.
 1101 *Space Weather*, 18 (8), e2020SW002467. <https://doi.org/10.1029/2020SW002467>
- 1102 Kelley, M. C. (2009). *The Earth's Ionosphere*. London, United Kingdom: Academic Press.
- 1103 Kennel, C. F., Edmiston, J. P., & Hada, T. (1985). A quarter century of collisionless shock
 1104 research. In R. G. Stone & B. Tsurutani (Eds.), *Collisionless Shocks in the Heliosphere:*
 1105 *A Tutorial Review*, Geophysical Monograph Series (Vol. 34, p. 1-36). Washington, D.C.:
 1106 American Geophysical Union. <https://doi.org/10.1029/GM034p0001>
- 1107 Kilpua, E. K. J., Jian, L. K., Li, Y., Luhmann, J. G., & Russell, C. T. (2011). Multipoint ICME
 1108 encounters: Pre-STEREO and STEREO observations. *Journal of Atmospheric and Solar-*
 1109 *Terrestrial Physics*, 73 (10), 1228-1241. <https://doi.org/10.1016/j.jastp.2010.10.012>
- 1110 Kilpua, E. K. J., Lumme, K., E. Andréevová, Isavnin, A., & Koskinen, H. E. J. (2015). Properties
 1111 and drivers of fast interplanetary shocks near the orbit of the Earth (1995-2013). *Journal*
 1112 *of Geophysical Research: Space Physics*, 120 (6), 4112–4125.
 1113 <https://doi.org/10.1002/2015JA021138>
- 1114 Kilpua, E. K. J., Fontaine, D., Moissard, C., Ala-Lahti, M., Palmerio, E., Yordanova, E., Good,
 1115 S. W., Kalliokoski, M. M. H., Lumme, E., Osmane, A., Palmroth, M., & Turc, L. (2019).
 1116 Solar Wind Properties and Geospace Impact of Coronal Mass Ejection-Driven Sheath
 1117 Regions: Variation and Driver Dependence. *Space Weather*, 17 (8), 1257-1280.
 1118 <https://doi.org/10.1029/2019SW002217>
- 1119 Kistler, L. M., Asamura, K., Kasahara, S., Miyoshi, Y., Mouikis, C. G., Keika, K., Petrinec, S.
 1120 M., Stevens, M. L., Hori, T., Yokota, S., & Shinohara, I. (2023). The variable source of
 1121 the plasma sheet during a geomagnetic storm. *Nature Communications*, 14(6143).
 1122 <https://doi.org/10.1038/s41467-023-41735-3>
- 1123 Kovář, P., & Sommer, M. (2020). CubeSat Observation of the Radiation Field of the South
 1124 Atlantic Anomaly. *Remote Sensing*, 13(7), 1274. <https://doi.org/10.3390/rs13071274>

- 1125 Kruparova, O., Maksimovic, M., Šafránková, Nĕmeček, Z., Santolik, O., & Krupar, V. (2013).
 1126 Automated interplanetary shock detection and its application to Wind observations.
 1127 *Journal of Geophysical Research*, 118 (8), 4793-4803. <https://doi.org/10.1002/jgra.50468>
- 1128 Laker, R., Horbury, T. S., O'Brien, H., Fauchon-Jones, E. J., Angelini, V., Fargette, N.,
 1129 Amerstorfer, T., Bauer, M., Möstl, C., Davies, E. E., Davies, J. A., Harrison, R., Barnes,
 1130 D., & Dumbović, M. (2024). Using Solar Orbiter as an Upstream Solar Wind Monitor for
 1131 Real Time Space Weather Predictions. *Space Weather*, 22 (2), e2023SW003628.
 1132 <https://doi.org/10.1029/2023SW003628>
- 1133 Laundal, K. M., & Richmond, A. D. (2017). Magnetic coordinate systems. *Space Science*
 1134 *Reviews*, 206(1-4), 1–33. <https://doi.org/10.1007/s11214-016-0275-y>
- 1135 Laundal, K. M., Reistad, J. P., Hatch, S. M., Madelaire, M., Walker, S., Hovland, A. Ø., Ohma,
 1136 A., Merkin, V. G., & Sorathia, K. A. (2022). Local Mapping of Polar Ionospheric
 1137 Electrodynamic. *Journal of Geophysical Research: Space Physics*, 127(5),
 1138 e2022JA030356. <https://doi.org/10.1029/2022JA030356>
- 1139 Ledvina, V. E., Palmerio, E., McGranaghan, R. M., Halford, A. J., Thayer, A., Brandt, L.,
 1140 MacDonald, E. A., Bhaskar, A., Dong, C., Altintas, I., Colliander, J., Jin, M., Jain, R. N.,
 1141 Chatterjee, S., Shaikh, Z., Frissell, N. A., Chen, T. Y., French, R. J., Isola, B., McIntosh,
 1142 S. W., Mason, E. I., Riley, P., Young, T., Barkhouse, W., Kazachenko, M. D., Snow, M.,
 1143 Ozturk, D. S., Claudepierre, S. G., Di Mare, F., Witteman, A., & Kuzub, J. (2022). How
 1144 open data and interdisciplinary collaboration improve our understanding of space
 1145 weather: A risk and resiliency perspective. *Frontiers in Astronomy and Space Science*,
 1146 9(1067571). <https://doi.org/10.3389/fspas.2022.1067571>
- 1147 Licata, R. J., & Mehta, P. M. (2022). Uncertainty quantification techniques for data- driven space
 1148 weather modeling: thermospheric density application. *Scientific Reports*, 12 (7256).
 1149 <https://doi.org/10.1038/s41598-022-11049-3>
- 1150 Lichtenberger, J., Clilverd, M. A., Heilig, B., Vellante, M., Manninen, J., Rodger, C. J., Collier,
 1151 A. B., Jørgensen, A. M., Reda, J., Holzworth, R. H., Friedel, R., & Simon-Wedlund, M.
 1152 (2013). The plasmasphere during a space weather event: first results from the PLASMON
 1153 project. *Journal of Space Weather and Space Climate*, 3(A23), 13.
 1154 <https://doi.org/10.1051/swsc/2013045>
- 1155 Liu, Y. D., Luhmann, J. G., Möstl, C., Martinez-Oliveros, J. C., Bale, S. D., Lin, R. P., Harrison,
 1156 R. A., Temmer, M., Webb, D. F., & Odstroil, D. (2012). Interactions between coronal
 1157 mass ejections viewed in coordinated imaging and in situ observations. *The Astrophysical*
 1158 *Journal Letters*, 746(2), L15. <https://doi.org/10.1088/2041-8205/746/2/L15>
- 1159 Liu, C., Wang, X., Zhang, S., & Xie, C. (2019). Effects of Lateral Conductivity Variations on
 1160 Geomagnetically Induced Currents: H-Polarization. *IEEE Access*, 7, 6,310-6,318.
 1161 <https://doi.org/10.1109/ACCESS.2018.2889462>

- 1162 Liu, Z.-Y., Zong, Q.-G., Li, L., Feng, Z.-J., Sun, Y.-X., Yu, X.-Q., Wang, Y.-F., Liu, J.-J., & Hu,
 1163 Z.-J. (2024). The Impact of the South Atlantic Anomaly on the Aurora System.
 1164 *Geophysical Research Letters*, 51 (3), e2023GL107209.
 1165 <https://doi.org/10.1029/2023GL107209>
- 1166 Loto'aniu, P. T. M., Romich, K., Rowland, W., Codrescu, S., Biesecker, D., Johnson, J., Singer,
 1167 H. J., Szabo, A., & Stevens, M. (2022). Validation of the DSCOVR Spacecraft Mission
 1168 Space Weather Solar Wind Products. *Space Weather*, 20 (10), e2022SW003085.
 1169 <https://doi.org/10.1029/2022SW003085>
- 1170 Love, J. J., & Finn, C. A. (2011). The USGS Geomagnetism Program and Its Role in Space
 1171 Weather Monitoring. *Space Weather*, 9 (7). <https://doi.org/10.1029/2011SW000684>
- 1172 Lugaz, N., Manchester IV, W. B., & Gombosi, T. I. (2005). Numerical Simulation of the
 1173 Interaction of Two Coronal Mass Ejections from Sun to Earth. *The Astrophysical*
 1174 *Journal*, 634(1). <https://doi.org/10.1086/491782>
- 1175 Lühr, H., Maus, S., & Rother, M. (2004). Noon-time equatorial electrojet: Its spatial features as
 1176 determined by the CHAMP satellite. *Journal of Geophysical Research*, 109 (A1).
 1177 <https://doi.org/10.1029/2002JA009656>
- 1178 Mac Manus, D. H., Rodger, C. J., Dalzell, M., Thomson, A. W. P., Clilverd, M. A., Petersen, T.,
 1179 Wolf, M. M., Thomson, N. R., & Divett, T. (2017). Long-term geomagnetically induced
 1180 current observations in New Zealand: Earth return corrections and geomagnetic field
 1181 driver. *Space Weather*, 15 (8), 1020-1038. <https://doi.org/10.1002/2017SW001635>
- 1182 Mac Manus, D. H., Rodger, C. J., Ingham, M., Clilverd, M. A., Dalzell, M., Divett, T.,
 1183 Richardson, G. S., & Petersen, T. (2022). Geomagnetically Induced Current Model in
 1184 New Zealand Across Multiple Disturbances: Validation and Extension to Non-Monitored
 1185 Transformers. *Space Weather*, 20 (2), e2021SW002955.
 1186 <https://doi.org/10.1029/2021SW002955>
- 1187 Malandraki, O. E., & Crosby, N. B. (2017). Solar Energetic Particles and Space Weather:
 1188 Science and Applications. In O. E. Malandraki & N. B. Crosby (Eds.), *Solar particle*
 1189 *radiation storms forecasting and analysis* (Vol. 444, p. 1-26). Cham, Switzerland:
 1190 Springer. https://doi.org/10.1007/978-3-319-60051-2_1
- 1191 Mansilla, G. A. (2014). Solar Cycle and Seasonal Distribution of Geomagnetic Storms with
 1192 Sudden Commencement. *Earth Science Research*, 3 (1), 50-55.
 1193 <https://doi.org/10.5539/esr.v3n1p50>
- 1194 Marshall, R. A., Dalzell, M., Waters, C. L., Goldthorpe, P., & Smith, E. A. (2012).
 1195 Geomagnetically induced currents in the New Zealand power network. *Space Weather*,
 1196 10 (8). <https://doi.org/10.1029/2012SW000806>

- 1197 Matamba, T. M., Habarulema, J. B., & McKinnell, L.-A. (2015). Statistical analysis of the
1198 ionospheric response during geomagnetic storm conditions over South Africa using
1199 ionosonde and GPS data. *Space Weather*, 13 (9), 536-547.
1200 <https://doi.org/10.1002/2015SW001218>
- 1201 Mauk, B. H., Fox, N. J., Kanekal, S. G., Kessel, R. L., Sibeck, D. G., & Ukhorskiy, A. (2012).
1202 Science Objectives and Rationale for the Radiation Belt Storm Probes Mission. In N. Fox
1203 & J. L. Burch (Eds.), *The Van Allen Probes Mission*. Boston, MA: Springer.
1204 https://doi.org/10.1007/978-1-4899-7433-4_2
- 1205 McComas, D. J., Christian, E. R., Schwadron, N. A., Fox, N., Westlake, J., Allegrini, F., Baker,
1206 D. N., Biesecker, D., Bzowski, M., Clark, G., Cohen, C. M. S., Cohen, I., Dayeh, M. A.,
1207 Decker, R., de Nolfo, G. A., Desai, M. I., Ebert, R. W., Elliott, H. A., Fahr, H., Frisch, P.
1208 C., Funsten, H. O., Fuselier, S. A., Galli, A., Galvin, A. B., Giacalone, J., Gkioulidou, M.,
1209 Guo, F., Horanyi, M., Isenberg, P., Janzen, P., Kistler, L. M., Korreck, K., Kubiak, M. A.,
1210 Kucharek, H., Larsen, B. A., Leske, R. A., Lugaz, N., Luhmann, J., Matthaeus, W.,
1211 Mitchell, D., Moebius, E., Ogasawara, K., Reisenfeld, D. B., Richardson, J. D., Russell,
1212 C. T., Sokoł, J. M., Spence, H. E., Skoug, R., Sternovsky, Z., Swaczyna, P., Szalay, J.
1213 R., Tokumaru, M., Wiedenbeck, M. E., Wurz, P., Zank, G. P., & Zirnstein, E. J. (2018).
1214 Interstellar Mapping and Acceleration Probe (IMAP): A New NASA Mission. *Space*
1215 *Science Reviews*, 214(116). <https://doi.org/10.1007/s11214-018-0550-1>
- 1216 McGranaghan, R. M., Bhatt, A., Matsuo, T., Mannucci, A. J., Semeter, J. L., & Datta-Barua, S.
1217 (2017). Ushering in a new frontier in geospace through data science. *Journal of*
1218 *Geophysical Research: Space Physics*, 122 (12), 12,586-12,590.
1219 <https://doi.org/10.1002/2017JA024835>
- 1220 McIntosh, S. W., Chapman, S., Leamon, R. J., Egeland, R., & Watkins, N. W. (2020).
1221 Overlapping Magnetic Activity Cycles and the Sunspot Number: Forecasting Sunspot
1222 Cycle 25 Amplitude. *Solar Physics*, 295(163). [https://doi.org/10.1007/s11207-020-](https://doi.org/10.1007/s11207-020-01723-y)
1223 [01723-y](https://doi.org/10.1007/s11207-020-01723-y)
- 1224 McIntosh, S. W., Leamon, R. J., & Egeland, R. (2023). Deciphering solar magnetic activity: The
1225 (solar) hale cycle terminator of 2021. *Frontiers in Astronomy and Space Science*, 10
1226 (1050523). <https://doi.org/10.3389/fspas.2023.1050523>
- 1227 Mishra, W., Dave, K., Srivastava, N., & Teriaca, L. (2021). Multipoint remote and *in situ*
1228 observations of interplanetary coronal mass ejection structures during 2011 and
1229 associated geomagnetic storms. *Monthly Notices of the Royal Astronomical Society*,
1230 506(1), 1186–1197. <https://doi.org/10.1093/mnras/stab1721>
- 1231 Miyoshi, Y., Shinohara, I., Ukhorskiy, S., Claudepierre, S. G., Mitani, T., Takashima, T., Hori,
1232 T., Santolik, O., Kolmasova, I., Matsuda, S., Kasahara, Y., Teramoto, M., Katoh, Y.,
1233 Hikishima, M., Kojima, H., Kurita, S., Imajo, S., Higashio, N., Kasahara, S., Yokota, S.,
1234 Asamura, K., Kazama, Y., Wang, S.-Y., Jun, C.-W., Kasaba, Y., Kumamoto, A.,
1235 Tsuchiya, F., Shoji, M., Nakamura, S., Kitahara, M., Mat-suoka, A., Shiokawa, K., Seki,

- 1236 K., Nosé, M., Takahashi, K., Martinez-Calderon, C., Hospodarsky, G., Colpitts, C.,
 1237 Kletzing, C., Wygant, J., Spence, H., Baker, D. N., Reeves, G. D., Blake, J. B., &
 1238 Lanzerotti, L. (2022). Collaborative Research Activities of the Arase and Van Allen
 1239 Probes. *Space Science Reviews*, 218(38). <https://doi.org/10.1007/s11214-022-00885-4>
- 1240 Moldwin, M. B., & Tsu, J. S. (2016). Stormtime Equatorial Electrojet Ground-Induced Currents.
 1241 In T. Fuller-Rowell, E. Yizengaw, P. H. Doherty, & S. Basu (Eds.), *Ionospheric Space*
 1242 *Weather, Geophysical Monograph Series* (Vol. 220, p. 33-40). Washington, D.C.:
 1243 American Geophysical Union. <https://doi.org/10.1002/9781118929216.ch3>
- 1244 Moore, T. E., Peterson, W. K., Russell, C. T., Chandler, M. O., Collier, M. R., Collin, H. L.,
 1245 Craven, P. D., Fitzenreiter, R., Giles, B. L., & Pollock, C. J. (1999). Ionospheric mass
 1246 ejection in response to a CME. *Geophysical Research Letters*, 26(15), 2339-2342.
 1247 <https://doi.org/10.1029/1999GL900456>
- 1248 Möstl, C., Farrugia, C. J., Kilpua, E. K. J., Jian, L. K., Liu, Y., Eastwood, J. P., Harrison, R. A.,
 1249 Webb1, D. F., Temmer, M., Odstrcil, D., Davies, J. A., Rollett, T., Luhmann, J. G.,
 1250 Nitta1, N., Mulligan, T., Jensen, E. A., Forsyth, R., Lavraud, B., de Koning, C. A.,
 1251 Veronig, A. M., Galvin, A. B., Zhang, T. L., & Anderson, B. J. (2012). Multi- point
 1252 shock and flux rope analysis of multiple interplanetary coronal mass ejections around
 1253 2010 august 1 in the inner heliosphere. *The Astrophysical Journal*, 758 (1), 10.
 1254 <https://doi.org/10.1088/0004-637X/758/1/10>
- 1255 Müller, D., St. Cyr, O. C., Zouganelis, I., Gilbert, H. R., Marsden, R., Nieves-Chinchilla, T.,
 1256 Antonucci, E., Auchère, F., Berghmans, D., Horbury, T. S., Howard, R. A., Krucker, S.,
 1257 Maksimovic, M., Owen, C. J., Rochus, P., Rodriguez-Pacheco, J., Romoli, M., Solanki,
 1258 S. K., Bruno, R., Carlsson, M., Fludra, A., Harra, L., Hassler, D. M., Livi, S., Louarn, P.,
 1259 Peter, H., Schühle, U., Teriaca, L., del Toro Iniesta, J. C., Wimmer-Schweingruber, R. F.,
 1260 Marsch, E., Velli, M., De Groof, A., Walsh, A., & Williams, D. (2020). The Solar Orbiter
 1261 mission. *Astronomy & Astrophysics*, 642 (A1), 31. <https://doi.org/10.1051/0004-6361/202038467>
- 1263 Nakamura, Y., Fukuda, S., Shibano, Y., Ogawa, H., ichiro Sakai, S., Shimizu, S., Soken, E.,
 1264 Miyazawa, Y., Toyota, H., Kukita, A., Maru, Y., Nakatsuka, J., Sakai, T., Takeuchi, S.,
 1265 Maki, K., Mita, M., Ogawa, E., Kakehashi, Y., Nitta, K., Asamura, K., Takashima, T., &
 1266 Shinohara, I. (2018). Exploration of energization and radiation in geospace (ERG):
 1267 challenges, development, and operation of satellite systems. *Earth, Planets and Space*,
 1268 70(102). <https://doi.org/10.1186/s40623-018-0863-z>
- 1269 Nandy, D. (2021). Progress in Solar Cycle Predictions: Sunspot Cycles 24–25 in Perspective.
 1270 *Solar Physics*, 296(54). <https://doi.org/10.1007/s11207-021-01797-2>
- 1271 Nandy, D., Martens, P. C. H., Obridko, V., Dash, S., & Georgieva, K. (2021). Solar evolution
 1272 and extrema: current state of understanding of long-term solar variability and its
 1273 planetary impacts. *Progress in Earth and Planetary Science*, 8(40).
 1274 <https://doi.org/10.1186/s40645-021-00430-x>

- 1275 Nandy, D., Baruah, Y., Bhowmik, P., Dash, S., Gupta, S., Hazra, S., Pal, B. L. S., Pal, S., Roy,
1276 S., Saha, C., & Sinha, S. (2023). Causality in heliophysics: Magnetic fields as a bridge
1277 between the Sun's interior and the Earth's space environment. *Journal of Atmospheric*
1278 *and Solar-Terrestrial Physics*, 248 , 106081. <https://doi.org/10.1016/j.jastp.2023.106081>
- 1279 Ness, N. F., & Wilcox, J. M. (1964). Solar Origin of the Interplanetary Magnetic Field. *Physics*
1280 *Review Letters*, 13(15), 461. <https://doi.org/10.1103/PhysRevLett.13.461>
- 1281 Ngwira, C. M., Sibeck, D., Silveira, M. V. D., Georgiou, M., Weygand, J. M., Nishimura, Y., &
1282 Hampton, D. (2018). A Study of Intense Local dB/dt Variations During Two
1283 Geomagnetic Storms. *Space Weather*, 16 (6), 676-693.
1284 <https://doi.org/10.1029/2018SW001911>
- 1285 Nilam, B., & Tulasi Ram, S. (2022). Large Geomagnetically Induced Currents at Equator Caused
1286 by an Interplanetary Magnetic Cloud. *Space Weather*, 20 (6), e2022SW003111.
1287 <https://doi.org/10.1029/2022SW003111>
- 1288 Nilam, B., Tulasi Ram, S., Ankita, M., Oliveira, D. M., & Dimri, A. P. (2023). Equatorial
1289 Electrojet (EEJ) response to Interplanetary (IP) shocks. *Journal of Geophysical*
1290 *Research: Space Physics*, 128(12). <https://doi.org/10.1029/2023JA032010>
- 1291 Nykyri, K., Ma, X., Burkholder, B., Liou, Y.-L., Cuéllar, R., Borovsky, S. K. J. E., Parker, J., De
1292 Moudt, M. R. L., Ebert, R. W., Ogasawara, K., Opher, M., Di Matteo, D. G. S. S., Viall,
1293 N., Wallace, S., Jorgensen, T. M., Hesse, M., Adhikari, M. J. W. L., Argall, M. R.,
1294 Egedal, J., Wilder, F., Broll, J., Poh, G., Wing, S., & Russell17, C. (2023). Seven Sisters:
1295 a mission to study fundamental plasma physical processes in the solar wind and a
1296 pathfinder to advance space weather prediction. *Frontiers in Astronomy and Space*
1297 *Science*, 10. <https://doi.org/10.3389/fspas.2023.1179344>
- 1298 Oh, S. Y., Yi, Y., & Kim, Y. H. (2007). Solar cycle variation of the interplanetary forward shock
1299 drivers observed at 1 AU. *Solar Physics*, 245(2), 391–410.
1300 <https://doi.org/10.1007/s11207-007-9042-2>
- 1301 Oliveira, D. M., & Raeder, J. (2015). Impact angle control of interplanetary shock
1302 geoeffectiveness: A statistical study. *Journal of Geophysical Research: Space Physics*,
1303 120(6), 4313-4323. <https://doi.org/10.1002/2015JA021147>
- 1304 Oliveira, D. M., & Ngwira, C. M. (2017). Geomagnetically Induced Currents: Principles.
1305 *Brazilian Journal of Physics*, 47(5), 552-560. <https://doi.org/10.1007/s13538-017-0523-y>
- 1306 Oliveira, D. M., & Samsonov, A. A. (2018). Geoeffectiveness of interplanetary shocks controlled
1307 by impact angles: A review. *Advances in Space Research*, 61(1), 1-44.
1308 <https://doi.org/10.1016/j.asr.2017.10.006>
- 1309 Oliveira, D. M., Arel, D., Raeder, J., Zesta, E., Ngwira, C. M., Carter, B. A., Yizengaw, E.,
1310 Halford, A. J., Tsurutani, B. T., & Gjerloev, J. W. (2018). Geomagnetically induced

- 1311 currents caused by interplanetary shocks with different impact angles and speeds. *Space*
 1312 *Weather*, 16 (6), 636-647. <https://doi.org/10.1029/2018SW001880>
- 1313 Oliveira, D. M., Hartinger, M. D., Xu, Z., Zesta, E., Pilipenko, V. A., Giles, B. L., & Silveira, M.
 1314 V. D. (2020). Interplanetary shock impact angles control magnetospheric ULF wave
 1315 activity: Wave amplitude, frequency, and power spectra. *Geophysical Research Letters*,
 1316 47(24), e2020GL090857. <https://doi.org/10.1029/2020GL090857>
- 1317 Oliveira, D. M., Weygand, J. M., Zesta, E., Ngwira, C. M., Hartinger, M. D., Xu, Z., Giles, B. L.,
 1318 Gershman, D. J., Silveira, M. V. D., & Souza, V. M. (2021). Impact angle control of local
 1319 intense dB/dt variations during shock-induced substorms. *Space Weather*, 19(12),
 1320 e2021SW002933. <https://doi.org/10.1029/2021SW002933>
- 1321 Oliveira, D. M. (2023a). Interplanetary Shock Data Base. *Frontiers in Astronomy and Space*
 1322 *Science*, 10. <https://doi.org/10.3389/fspas.2023.1240323>
- 1323 Oliveira, D. M. (2023b). Geoeffectiveness of Interplanetary Shocks Controlled by Impact
 1324 Angles: Past Research, Recent Advancements, and Future Work. *Frontiers in Astronomy*
 1325 *and Space Science*, 10. <https://doi.org/10.3389/fspas.2023.1179279>
- 1326 Oliveira, D. M. (2023c). *Interplanetary shock data base*. [Data Set]. (Version 1). Zenodo.
 1327 <https://doi.org/10.5281/zenodo.7991430>
- 1328 Oliveira, D. M., Weygand, J. M., Coxon, J. C., & Zesta, E. (2024a). Impact Angle Control of
 1329 Local Intense dB/dt Variations During Shock-Induced Substorms: A Statistical Study.
 1330 *Space Weather*, 22, e2023SW003767. <https://doi.org/10.1029/2023SW003767>
- 1331 Oliveira, D. M., Zesta, E., & Vidal-Luengo, S. (2024b). First direct observations of inter-
 1332 planetary shock impact angle effects on actual geomagnetically induced currents: The
 1333 case of the Finnish natural gas pipeline system. *Frontiers in Astronomy and Space*
 1334 *Science*, 11. <https://doi.org/10.3389/fspas.2024.1392697>
- 1335 Omidi, N., Zhou, X.-Z., Russell, C. T., & Angelopoulos, V. (2023). Interaction of Interplanetary
 1336 Shocks with the Moon: Hybrid Simulations and ARTEMIS observations. *Journal of*
 1337 *Geophysical Research: Space Physics*, 128 (6), e2022JA030499.
 1338 <https://doi.org/10.1029/2022JA030499>
- 1339 Oughton, E. J., Skelton, A., Horne, R. B., Thomson, A. W. P., & Gaunt, C. T. (2017).
 1340 Quantifying the daily economic impact of extreme space weather due to failure in
 1341 electricity transmission infrastructure. *Space Weather*, 15 (1), 65–83.
 1342 <https://doi.org/10.1002/2016SW001491>
- 1343 Owens, M. J., Lockwood, M., Barnard, L. A., Scott, C. J., Haines, C., & Macneil, A. (2021).
 1344 Extreme Space-Weather Events and the Solar Cycle. *Solar Physics*, 296(82).
 1345 <https://doi.org/10.1007/s11207-021-01831-3>

- 1346 Paterson, W. R., Gershman, D. J., Kanekal, S. G., Livi, R., Moldwin, M. B., Randol, B., Samara,
1347 M., & Zesta, E. (2021). The HERMES Space-Weather Science Payload for Gateway. In
1348 *Final Paper Abstract Number: P51B-04*. Presented at the 2021 AGU Fall Meeting, New
1349 Orleans, LA, 13-17 Dec.
- 1350 Patterson, C. J., Wild, J. A., & Boteler, D. H. (2023). Modeling the Impact of Geomagnetically
1351 Induced Currents on Electrified Railway Signaling Systems in the United Kingdom.
1352 *Space Weather*, 21 (3), e2022SW003385. <https://doi.org/10.1029/2022SW003385>
- 1353 Pavón-Carrasco, F. J., & De Santis, A. (2016). The South Atlantic Anomaly: The Key for a
1354 Possible Geomagnetic Reversal. *Frontiers in Earth Sciences*, 4.
1355 <https://doi.org/10.3389/feart.2016.00040>
- 1356 Pedregosa, F., Varoquaux, G., Gramfort, A., Michel, V., Thirion, B., Grisel, O., Blondel, M.,
1357 Prettenhofer, P., Weiss, R., Dubourg, V., Vanderplas, J., Passos, A., Cournapeau, D.,
1358 Brucher, M., Perrot, M., & Duchesnay, E. (2011). Scikit-learn: Machine Learning in
1359 Python. *Journal of Machine Learning Research*, 12, 2825–2830.
- 1360 Pesnell, W. D. (2015). Predictions of solar cycle 24: How are we doing? *Space Weather*, 14(1),
1361 10-21. <https://doi.org/10.1002/2015SW001304>
- 1362 Peterson, W. K., Andersson, L., Callahan, B. C., Collin, H. L., Scudder, J. D., & Yau, A. W.
1363 (2008). Solar-minimum quiet time ion energization and outflow in dynamic boundary
1364 related coordinates. *Journal of Geophysical Research*, 113(A7).
1365 <https://doi.org/10.1029/2008JA013059>
- 1366 Piersanti, M., Di Matteo, S., Carter, B. A., Currie, J., & D’Angelo, G. (2019). Geoelectric Field
1367 Evaluation During the September 2017 Geomagnetic Storm: MA.I.GIC. Model. *Space*
1368 *Weather*, 17(8), 1241-1256. <https://doi.org/10.1029/2019SW002202>
- 1369 Piersanti, M., Del Moro, D., Parmentier, A., Martucci, M., Palma, F., Sotgiu, A., Plainaki, C.,
1370 D’Angelo, G., Berrilli, F., Recchiuti, D., Papini, E., Giovannelli, L., Napoletano, G.,
1371 Iuppa, R., Diego, P., Cicone, A., Mergé, M., De Donato, C., De Santis, C., Sparvoli, R.,
1372 Ubertini, P., Battiston, R., & Picozza, P. (2022). On the Magnetosphere- Ionosphere
1373 Coupling During the May 2021 Geomagnetic Storm. *Space Weather*, 20 (6),
1374 e2021SW003016. <https://doi.org/10.1029/2021SW003016>
- 1375 Pitout, F., Marchaudon, A., Blelly, P.-L., Bai, X., Forme, F., Buchert, S. C., & Lorentzen, D. A.
1376 (2015). Swarm and ESR observations of the ionospheric response to a field- aligned
1377 current system in the high-latitude midnight sector. *Geophysical Research Letters*,
1378 42(11), 4270-4279. <https://doi.org/10.1002/2015GL064231>
- 1379 Pulkkinen, A., Kuznetsova, K., Ridley, A., Raeder, J., Vapirev, A., Weimer, D., Weigel, R. S.,
1380 Wiltberger, M., Millward, G., Rastätter, L., Hesse, M., Singer, H. J., & Chulaki, A.
1381 (2011). Geospace environment modeling 2008-2009 challenge: Ground magnetic field
1382 perturbations. *Space Weather*, 9 (2). <https://doi.org/10.1029/2010SW000600>

- 1383 Pulkkinen, A., Rastatter, L., Kuznetsova, M., Singer, H., Balch, C., Weimer, D., Tóth, G.,
 1384 Ridley, A., Gombosi, T., Wiltberger, M., Raeder, J., & Weigel, R. (2013). Community-
 1385 wide validation of geospace model ground magnetic field perturbation predictions to
 1386 support model transition to operations. *Space Weather*, 11(6), 369-385.
 1387 <https://doi.org/10.1002/swe.20056>
- 1388 Pulkkinen, A., Bernabeu, E., Thomson, A., Viljanen, A., Pirjola, R., Boteler, D., Eichner, J.,
 1389 Cilliers, P. J., Welling, D., Savani, N. P., Weigel, R. S., Love, J. J., Balch, C., Ngwira, C.
 1390 M., Crowley, G., Schultz, A., Kataoka, R., Anderson, B., Fugate, D., Simpson, J. J., &
 1391 MacAlester, M. (2017). Geomagnetically induced currents: Science, engineering, and
 1392 applications readiness. *Space Weather*, 15 (7), 828-856.
 1393 <https://doi.org/10.1002/2016SW001501>
- 1394 Richardson, I. G., Webb, D. F., Zhang, J., Berdichevsky, D. B., Biesecker, D. A., Kasper, J. C.,
 1395 Kataoka, R., Steinberg, J. T., Thompson, B. J., Wu, C.-C., & Zhukov, A. N. (2006).
 1396 Major geomagnetic storms ($Dst \leq -100$ nT) generated by corotating interaction regions.
 1397 *Journal of Geophysical Research*, 111 (A7). <https://doi.org/10.1029/2005JA011476>
- 1398 Richardson, I. G. (2018). Solar wind stream interaction regions throughout the heliosphere.
 1399 *Living Reviews in Solar Physics*, 15 (1). <https://doi.org/10.1007/s41116-017-0011-z>
- 1400 Reames, D. V. (1999). Particle acceleration at the sun and in the heliosphere. *Space Science*
 1401 *Reviews*, 9(3), 413–491. <https://doi.org/10.1023/A:1005105831781>
- 1402 Rodger, C. J., Mac Manus, D. H., Dalzell, M., Thomson, A. W. P., Clarke, E., Petersen, T.,
 1403 Clilverd, M. A., & Divett, T. (2017). Long-Term Geomagnetically Induced Current
 1404 Observations From New Zealand: Peak Current Estimates for Extreme Geomagnetic
 1405 Storms. *Space Weather*, 15 (11), 1447-1460. <https://doi.org/10.1002/2017SW001691>
- 1406 Rong, S., & Bao-wen, Z. (2018). The research of regression model in machine learning field.
 1407 *MATEC Web Conf.*, 176, 01033. <https://doi.org/10.1051/mateccconf/201817601033>
- 1408 Rowland, D., Halford, A., Klenzing, J., Pfaff, R., Oliveira, D., Paxton, L., Turner, D.,
 1409 Verkhoglyadova, O., & Zou, S. (2023). Cross-Scale and Cross-Regime Coupling in the
 1410 ITM: Studying Weather, not just Climate, in the Middle and Upper Atmosphere. *Bulletin*
 1411 *of the AAS*, 55(3). <https://doi.org/10.3847/25c2cfef.041166a2>
- 1412 Russell, C. T., Ginskey, M., & Petrinec, S. M. (1994). Sudden impulses at low-latitude stations:
 1413 Steady state response for northward interplanetary magnetic field. *Journal of*
 1414 *Geophysical Research*, 99(A1), 253–261. <https://doi.org/10.1029/93JA02288>
- 1415 Sai Gowtam, V., Tulasi Ram, S., Reinisch, B., & Prajapati, A. (2019). A New Artificial Neural
 1416 Network-Based Global Three-Dimensional Ionospheric Model (ANNIM-3D) Using
 1417 Long-Term Ionospheric Observations: Preliminary Results. *Journal of Geophysical*
 1418 *Research: Space Physics*, 124(6), 4639-4657. <https://doi.org/10.1029/2019JA026540>

- 1419 Schaefer, R. K., Paxton, L. J., Selby, C., Ogorzalek, B., Romeo, G., Wolven, B., & Hsieh, S.-Y.
 1420 (2016). Observation and modeling of the South Atlantic Anomaly in low Earth orbit
 1421 using photometric instrument data. *Space Weather*, 14 (5), 330-342.
 1422 <https://doi.org/10.1002/2016SW001371>
- 1423 Schiller, Q., Kanekal, S. G., Jian, L. K., Li, X., Jones, A., Baker, D. N., Jaynes, A., & Spence, H.
 1424 E. (2016). Prompt injections of highly relativistic electrons induced by interplanetary
 1425 shocks: A statistical study of Van Allen Probes observations. *Geophysical Research*
 1426 *Letters*, 43(24), 12,317-12,324. <https://doi.org/10.1002/2016GL071628>
- 1427 Shirky, C. (2010). *Cognitive surplus: Creativity and generosity in a connected age*. London,
 1428 United Kingdom: Penguin.
- 1429 Silva, G. B. D., Alves, L. R., Espinosa, K. V., Souza, V. M., da Silva, L. A., Costa, J. E. R.,
 1430 Pádua, M. B., & Sanchez, S. A. (2024). Evaluation of dB/dt amplitudes and sources over
 1431 the Brazilian region during geomagnetic storms in the 2021–2022 biennium. *Journal of*
 1432 *Atmospheric and Solar-Terrestrial Physics*. <https://doi.org/10.1016/j.jastp.2024.106196>
- 1433 Silverman, S. M. (1995). Low latitude auroras: the storm of 25 September 1909. *Journal of*
 1434 *Atmospheric and Solar-Terrestrial Physics*, 57 (6), 673-685.
 1435 [https://doi.org/10.1016/0021-9169\(94\)E0012-C](https://doi.org/10.1016/0021-9169(94)E0012-C)
- 1436 Smith, E. J., & Wolfe, J. H. (1976). Observations of interaction regions and corotating shocks
 1437 between one and five AU: Pioneers 10 and 11. *Geophysical Research Letters*, 3(3), 137–
 1438 140. <https://doi.org/10.1029/GL003i003p00137>
- 1439 Smith, E. J., Tsurutani, B. T., & Rosenberg, R. L. (1978). Observations of the interplanetary
 1440 sector structure up to heliographic latitudes of 16°: Pioneer 11. *Journal of Geophysical*
 1441 *Research*, 83(A2), 717-724. <https://doi.org/10.1029/JA083iA02p00717>
- 1442 Smith, E. J., Slavin, J. A., Zwickl, R. D., & Bame, S. J. (1986). Shocks and storm sudden
 1443 commencements. In Y. Kamide & J. A. Slavin (Eds.), *Solar wind and magnetosphere*
 1444 *coupling* (p. 345). Tokyo, Japan: Terra Scientific.
- 1445 Smith, A. W., Rae, J., Forsyth, C., Oliveira, D. M., Freeman, P. M., & Jackson, D. (2020a).
 1446 Probabilistic Forecasts of Storm Sudden Commencements from Interplanetary Shocks
 1447 using Machine Learning. *Space Weather*, 18 (11), e2020SW002603.
 1448 <https://doi.org/10.1029/2020SW002603>
- 1449 Smith, M., Craig, D., Herrmann, N., Mahoney, E., Krezel, J., McIntyre, N., & Goodliff, K.
 1450 (2020b). The Artemis Program: An Overview of NASA’s Activities to Return Humans to
 1451 the Moon. In *2020 IEEE Aerospace Conference* (p. 1-10). Big Sky, MT.
 1452 <https://doi.org/10.1109/AERO47225.2020.9172323>
- 1453 Smith, A. W., Rodger, C. J., Mac Manus, D. H., Forsyth, C., Rae, I. J., Freeman, M. P., Clilverd,
 1454 M. A., Petersen, T., & Dalzell, M. (2022). The Correspondence Between Sudden

- 1455 Commencements and Geomagnetically Induced Currents: Insights From New Zealand.
1456 *Space Weather*, 20(8), e2021SW002983. <https://doi.org/10.1029/2021SW002983>
- 1457 Smith, A. W., Rodger, C. J., Mac Manus, D. H., Rae, I. J., Fogg, A. R., Forsyth, C., Fisher, P.,
1458 Petersen, T., & Dalzell, M. (2024). Sudden Commencements and Geomagnetically
1459 Induced Currents in New Zealand: Correlations and Dependence. *Space Weather*, 22(1),
1460 e2023SW003731. <https://doi.org/10.1029/2023SW003731>
- 1461 Somasundaram, S., & Megala, S. (2017). Aditya-L1 mission. *Current Science*, 11 (4), 610-613.
1462 <https://doi.org/10.18520/cs/v113/i04/610-612>
- 1463 Srivastava, N., Mishra, W., & Chakrabarty, D. (2018). Interplanetary and Geomagnetic
1464 Consequences of Interacting CMEs of 13-14 June 2012. *Solar Physics*, 293 (5).
1465 <https://doi.org/10.1007/s11207-017-1227-8>
- 1466 Stephenson, F. R. (1990). Historical Evidence concerning the Sun: Interpretation of Sunspot
1467 Records during the Telescopic and Pretelescopic Eras. *Philosophical Transactions of the*
1468 *Royal Society of London. Series A*, 330(1615), 499-512.
1469 <https://doi.org/10.1098/rsta.1990.0031>
- 1470 Stone, E. C., Frandsen, A. M., Mewaldt, R. A., Christian, E. R., Margolies, D., Ormes, J. F., &
1471 Snow, F. (1998). The Advanced Composition Explorer. *Space Science Reviews*, 86(1-4),
1472 1-22. <https://doi.org/10.1023/A:1005082526237>
- 1473 Tapping, K., & Morgan, C. (2017). Changing Relationships Between Sunspot Number, Total
1474 Sunspot Area and F10.7 in Cycles 23 and 24. *Solar Physics*, 292(73), 1-14.
1475 <https://doi.org/10.1007/s11207-017-1111-6>
- 1476 Thaduri, A., Galar, D., & Kumar, U. (2020). Space weather climate impacts on railway
1477 infrastructure. *International Journal of System Assurance Engineering and Management*,
1478 11(Suppl 2), 267-281. <https://doi.org/10.1007/s13198-020-01003-9>
- 1479 Torta, J. M., Marcuello, A., Campanyà, J., Marsal, S., Queralt, P., & Ledo, J. (2017). Improving
1480 the modeling of geomagnetically induced currents in Spain. *Space Weather*, 15(5), 691-
1481 703. <https://doi.org/10.1002/2017SW001628>
- 1482 Townsend, L. W., Wilson, J. W., Shinn, J. L., & S. B, C. (1992). Human exposure to large solar
1483 particle events in space. *Advances in Space Research*, 12(2-3), 339-348.
1484 [https://doi.org/10.1016/0273-1177\(92\)90126-i](https://doi.org/10.1016/0273-1177(92)90126-i)
- 1485 Tozzi, R., De Michelis, P., Coco, I., & Giannattasio, F. (2019). A Preliminary Risk Assessment
1486 of Geomagnetically Induced Currents over the Italian Territory. *Space Weather*, 17(1),
1487 46-58. <https://doi.org/10.1029/2018SW002065>
- 1488 Tripathi, D., Chakrabarty, D., Nandi, A., Prasad, B. R., Ramaprakash, A. N., Shaji, N.,
1489 Sankarasubramanian, K., Thampi, R. S., & Yadav, V. K. (2023). The Aditya-L1 mission

- 1490 of ISRO. In G. Cauzzi & A. Tritschler (Eds.), *The Era of Multi-Messenger Solar Physics*
 1491 (Vol. 18). Cambridge University Press. <https://doi.org/10.1017/S1743921323001230>
- 1492 Tsurutani, B. T., & Lin, R. P. (1985). Acceleration of > 47 keV ions and > 2 keV electrons by
 1493 interplanetary shocks at 1 AU. *Journal of Geophysical Research*, 90(A1), 1–11.
 1494 <https://doi.org/10.1029/JA090iA01p00001>
- 1495 Tsurutani, B. T., Gonzalez, W. D., Gonzalez, A. L. C., Tang, F., Arballo, J. K., & Okada, M.
 1496 (1995). Interplanetary origin of geomagnetic activity in the declining phase of the solar
 1497 cycle. *Journal of Geophysical Research*, 100(A11), 21717-21733.
 1498 <https://doi.org/10.1029/95JA01476>
- 1499 Tsurutani, B., Mannucci, A., Iijima, B., Abdu, M. A., Sobral, J. H. A., Gonzalez, W., Guarnieri,
 1500 F., Tsuda, T., Saito, A., Yumoto, K., Fejer, B., Fuller-Rowell, T. J., Kozyra, J., Foster, J.
 1501 C., Coster, A., & Vasyliunas, V. M. (2004). Global dayside ionospheric uplift and
 1502 enhancement associated with interplanetary electric fields. *Journal of Geophysical*
 1503 *Research*, 109(A8). <https://doi.org/10.1029/2003JA010342>
- 1504 Tsurutani, B. T., Lakhina, G. S., Verkhoglyakova, O. P., Gonzalez, W. D., Echer, E., &
 1505 Guarnieri, F. L. (2011). A review of interplanetary discontinuities and their geomagnetic
 1506 effects. *Journal of Atmospheric and Solar-Terrestrial Physics*, 73(1), 5-19.
 1507 <https://doi.org/10.1016/j.jastp.2010.04.001>
- 1508 Tsurutani, B. T., Hajra, R., Echer, E., & Gjerloev, J. W. (2015). Extremely intense (SML \leq
 1509 -2500 nT) substorms: isolated events that are externally triggered? *Annales Geophysicae*,
 1510 33, 519-524. <https://doi.org/10.5194/angeo-33-519-2015>
- 1511 Tsurutani, B. T., & Hajra, R. (2021). The Interplanetary and Magnetospheric causes of
 1512 Geomagnetically Induced Currents (GICs) > 10 A in the Mäntsälä Finland Pipeline: 1999
 1513 through 2019. *Journal of Space Weather and Space Climate*, 11(23), 1-23.
 1514 <https://doi.org/10.1051/swsc/2021001>
- 1515 Tsurutani, B. T., & Hajra, R. (2023). Energetics of Shock-triggered Supersubstorms (SML < $-$
 1516 2500 nT). *The Astrophysical Journal*, 946 (17). [https://doi.org/10.3847/1538-](https://doi.org/10.3847/1538-4357/acb143)
 1517 [4357/acb143](https://doi.org/10.3847/1538-4357/acb143)
- 1518 Tulasi Ram, S., Nilam, B., Balan, N., Zhang, Q., Shiokawa, K., Chakrabarty, D., Xing, Z.,
 1519 Venkatesh, K., Veenadhari, B., & Yoshikawa, A. (2019). Three Different Episodes of
 1520 Prompt Equatorial Electric Field Perturbations Under Steady Southward IMF B_z During
 1521 St. Patrick's Day Storm. *Journal of Geophysical Research: Space Physics*, 124(12),
 1522 10428-10443. <https://doi.org/10.1029/2019JA027069>
- 1523 Upton, L. A., & Hathaway, D. H. (2023). Solar cycle precursors and the outlook for cycle 25.
 1524 *Journal of Geophysical Research: Space Physics*, 128(10), e2023JA031681.
 1525 <https://doi.org/10.1029/2023JA031681>

- 1526 Vaquero, J. M., & Vázquez, M. (2009). *The Sun Recorded Through History*. New York, NY:
1527 Springer. <https://doi.org/10.1007/978-0-387-92790-9>
- 1528 Vázquez, M., Vaquero, J. M., Gallego, M. C., Roca Cortés, T., & Pallé, R. L. (2016). Long-Term
1529 Trends and Gleissberg Cycles in Aurora Borealis Records (1600 – 2015). *Solar Physics*,
1530 291(2), 613-642. <https://doi.org/10.1007/s11207-016-0849-6>
- 1531 Vargas, M., Guerrero-Martin, E., Vassiliadis, D., Vollmer, J., Comeyne, G., Hanni, R., Floyd,
1532 M., Inskip, J., Azeem, I., & Talaat, E. R. (2024). The NOAA-NASA Space Weather
1533 Follow On (SWFO) Program to Sustain Operational Space-based Observations of Solar
1534 Wind and Coronal Mass Ejections. In Abstract number 423. American Meteorological
1535 Society, 104th Annual Meeting, Baltimore, MD, 28 January – 1 February 2024.
- 1536 Vernov, S. N., Gorchakov, E. V., Shavrin, P. I., & Sharvina, K. N. (1967). Radiation belts in the
1537 region of the South-Atlantic magnetic anomaly. *Space Science Reviews*, 7(4), 490-533.
1538 <https://doi.org/10.1007/BF00182684>
- 1539 Viljanen, A. (1998). Relation of geomagnetically induced currents and local geomagnetic
1540 variations. *IEEE Transactions on Power Delivery*, 13 (4), 1285-1290.
1541 <https://doi.org/10.1109/61.714497>
- 1542 Viljanen, A., Pirjola, R., Prácer, E., Katkalov, J., & Wik, M. (2014). Geomagnetically induced
1543 currents in Europe. *Journal of Space Weather and Space Climate*, 4(A9).
1544 <https://doi.org/10.1051/swsc/2014006>
- 1545 Villante, U., & Piersanti, M. (2011). Sudden impulses at geosynchronous orbit and at ground.
1546 *Journal of Atmospheric and Solar-Terrestrial Physics*, 73 (1), 61-76.
1547 <https://doi.org/10.1016/j.jastp.2010.01.008>
- 1548 Vines, S., Anderson, B., Waters, C. L., Allen, R. C., Maute, A., Kunduri, B., Paxton, L.,
1549 Strangeway, R. J., Lin, D., Robinson, R., Le, G., Zhu, Q., Milan, S., Ozturk, D., Korth,
1550 H., Laundal, K., Ohtani, S., Chartier, A., Murphy, K., Matsuo, T., Sotirelis, T., Knipp, D.,
1551 Califf, S., de Mesquita, R. L. A., Connor, H., James, C., & Gang, L. (2023). Beyond
1552 ampere-next: Envisioning the next system of global high-latitude electrodynamics.
1553 *Bulletin of the AAS*, 55(3). <https://doi.org/10.3847/25c2cf.76348bf9>
- 1554 Wang, Y. M., Ye, P. Z., Wang, S., & Xue, X. H. (2003). An interplanetary cause of large
1555 geomagnetic storms: Fast forward shock overtaking preceding magnetic cloud.
1556 *Geophysical Research Letters*, 30(13). <https://doi.org/10.1029/2002GL016861>
- 1557 Wang, C., Li, C. X., Huang, Z. H., & Richardson, J. D. (2006). Effect of interplanetary shock
1558 strengths and orientations on storm sudden commencement rise times. *Geophysical*
1559 *Research Letters*, 33(14), 1-3. <https://doi.org/10.1029/2006GL025966>
- 1560 Wang, C., Li, H., Richardson, J. D., & Kan, J. R. (2010a). Interplanetary shock characteristics
1561 and associated geosynchronous magnetic field variations estimated from sudden impulses

- 1562 observed on the ground. *Journal of Geophysical Research*, 115(A9).
 1563 <https://doi.org/10.1029/2009JA014833>
- 1564 Wawrzaszek, A., Gil, A., Modzelewska, R., Tsurutani, B. T., & Wawrzaszek, R. (2023).
 1565 Analysis of Large Geomagnetically Induced Currents During the 7–8 September 2017
 1566 Storm: Geoelectric Field Mapping. *Space Weather*, 21 (3), e2022SW003383.
 1567 <https://doi.org/10.1029/2022SW003383>
- 1568 Wilson III, L. B., Brosius, A. L., Gopalswamy, N., Nieves-Chinchilla, T., Szabo, A., Hurley, K.,
 1569 Phan, T., Kasper, J. C., Lugaz, N., Richardson, I. G., Chen, C. H. K., Verscharen, D.,
 1570 Wicks, R. T., & TenBarge, J. M. (2021). A Quarter Century of Wind Spacecraft
 1571 Discoveries. *Reviews of Geophysics*, 59 (2), e2020RG000714.
 1572 <https://doi.org/10.1029/2020RG000714>
- 1573 World Data Center for Geomagnetism, Kyoto, Nose, M., Iyemori, T., Sugiura, M., & Kamei, T.
 1574 (2015). *Geomagnetic Dst index*. [Data Set]. (Version v1). World Data Center.
 1575 <https://doi.org/10.17593/14515-74000>
- 1576 Yadav, V. K., Srivastava, N., Ghosh, S. S., Srikar, P. T., & Subhalakshmi, K. (2018). Science
 1577 objectives of the magnetic field experiment onboard Aditya-L1 spacecraft. *Advances in*
 1578 *Space Research*, 61(2), 749-758. <https://doi.org/10.1016/j.asr.2017.11.008>
- 1579 Yadav, V. K. (2020). Alfvén wave Detection at first Lagrangian Point with Magnetic Field
 1580 Measurements. *IETE Technical Review*, 37 (1).
 1581 <https://doi.org/10.1080/02564602.2018.1541767>
- 1582 Yee, J. H., Gjerloev, J., Wu, D., & Schwartz, M. J. (2017). First Application of the Zeeman
 1583 Technique to Remotely Measure Auroral Electrojet Intensity From Space. *Geophysical*
 1584 *Research Letters*, 44(20), 10,134-10,139. <https://doi.org/10.1002/2017GL074909>
- 1585 Yee, J. H., Gjerloev, J., & Wu, D. (2021). Remote sensing of magnetic fields induced by
 1586 electrojets from space. In W. Wang, Y. Zhang, & L. J. Paxton (Eds.), *Measurement*
 1587 *Techniques and Sensor Design*, Geophysical Monograph Series (p. 451-468).
 1588 Washington, D.C.: American Geophysical Union.
 1589 <https://doi.org/10.1002/9781119815631.ch21>
- 1590 Yue, C., Zong, Q. G., Zhang, H., Wang, Y. F., Yuan, C. J., Pu, Z. Y., Fu, S. Y., Lui, A. T. Y.,
 1591 Yang, B., & Wang, C. R. (2010). Geomagnetic activity triggered by interplanetary
 1592 shocks. *Journal of Geophysical Research*, 115(A00I05), 1–13.
 1593 <https://doi.org/10.1029/2010JA015356>
- 1594 Yue, C., Li, W., Nishimura, Y., Zong, Q., Ma, Q., Bortnik, J., Thorne, R. M., Reeves, G. D.,
 1595 Spence, H. E., Kletzing, C. A., Wygant, J. R., & Nicolls, M. J. (2016). Rapid
 1596 enhancement of low-energy (< 100 eV) ion flux in response to interplanetary shocks
 1597 based on two Van Allen Probes case studies: Implications for source regions and heating

- 1598 mechanisms. *Journal of Geophysical Research: Space Physics*, 121 (7), 6430-6443.
1599 <https://doi.org/10.1002/2016JA022808>
- 1600 Zeeman, P. (1897). On the influence of magnetism on the nature of the light emitted by a
1601 substance. *Philosophical Magazine*, 43 (262).
1602 <https://doi.org/10.1080/14786449708620985>
- 1603 Zhao, H. S., Liu, C. Z., Li, X. Q., Liao, J. Y., Zhang, J., Qu, J. L., Lu, F. J., Zhang, S. N., Song,
1604 L. M., Zhang, S., Li, T. P., Xu, Y. P., Cao, X. L., & Chen, Y. (2020). The observation of
1605 the South Atlantic Anomaly with the particle monitors onboard Insight-HXMT. *Journal*
1606 *of High Energy Astrophysics*, 26, 95-101. <https://doi.org/10.1016/j.jheap.2020.04.001>
- 1607 Zhao, K., Kistler, L. M., Lund, E. J., Nowrouzi, N., Kitamura, N., & Strangeway, R. J. (2020).
1608 Factors Controlling O⁺ and H⁺ Outflow in the Cusp During a Geomagnetic Storm:
1609 FAST/TEAMS Observations. *Geophysical Research Letters*, 47 (11), e2020GL086975.
1610 <https://doi.org/10.1029/2020GL086975>
- 1611 Zhou, X.-Y., & Tsurutani, B. T. (1999). Rapid intensification and propagation of the dayside
1612 aurora: Large scale interplanetary pressure pulses (fast shocks). *Geophysical Research*
1613 *Letters*, 26(8), 1097-1100. <https://doi.org/10.1029/1999GL900173>
- 1614 Zhou, X., & Tsurutani, B. T. (2001). Interplanetary shock triggering of nightside geomagnetic
1615 activity: Substorms, pseudobreakups, and quiescent events. *Journal of Geophysical*
1616 *Research*, 106(A9), 18957-18967. <https://doi.org/10.1029/2000JA003028>
- 1617 Zong, Q.-G., Wang, Y. F., Zhang, H., Fu, S. Y., Zhang, H., Wang, C. R., Yuan, C. J., &
1618 Vogiatzis, I. (2012). Fast acceleration of inner magnetospheric hydrogen and oxygen ions
1619 by shock induced ULF waves. *Journal of Geophysical Research*, 117(A11).
1620 <https://doi.org/10.1029/2012JA018024>
- 1621 Zong, Q.-G., Zhou, X.-Z., Wang, Y. F., Li, X., Song, P., Baker, D. N., Fritz, T. A., Daly, P. W.,
1622 Dunlop, M., & Pedersen, A. (2009). Energetic electron response to ULF waves induced
1623 by interplanetary shocks in the outer radiation belt. *Journal of Geophysical Research*,
1624 114(A10204), 1-13. <https://doi.org/10.1029/2009JA014393>
- 1625 Zong, Q.-G., Yue, C., & Fu, S. Y. (2021). Shock Induced Strong Substorms and Super
1626 Substorms: Preconditions and Associated Oxygen Ion Dynamics. *Space Science Reviews*,
1627 217 (33). <https://doi.org/10.1007/s11214-021-00806-x>